Genome-wide RNAi screen identifies Romo1 as a novel regulator of mitochondrial fusion and cristae integrity

Matthew Norton

This thesis is submitted as a partial fulfillment of the M. Sc program in

Cellular and Molecular Medicine

28 September 2012

Department of Cellular and Molecular Medicine

Faculty of Medicine

University of Ottawa

Abstract

Mitochondria exist in a dynamic network regulated by the opposing processes of mitochondrial fusion and fission. Regulation of mitochondrial morphology is critical for metabolism, quality control and cell survival, among other cellular processes. Large GTPases are responsible for shaping the mitochondrial network. Mitofusins 1 and 2 and Opa1 regulate outer and inner mitochondrial membrane fusion, respectively. Conversely, Drp1 is recruited to mitochondria to carry out fission. Although many proteins have been implicated in these processes, there are still many unknowns. We sought to identify novel regulators of mitochondrial morphology and conducted a genome-wide RNAi screen to identify candidate genes. We identified Reactive Oxygen species Modulator 1 (ROMO1) as a novel regulator of mitochondrial fusion and cristae integrity. In the absence of ROMO1, the mitochondrial network fragments and cristae are lost. These defects lead to impaired mitochondrial respiration and sensitization to cytochrome c release and downstream apoptosis. ROMO1 is regulated by mitochondrial REDOX at 4 cysteine residues that couple REDOX signaling to mitochondrial morphology. We have characterized ROMO1 as an interactor with the MINOS complex, required for cristae junction maintenance, and the inner mitochondrial membrane fusion GTPase OPA1. Through these interactions ROMO1 couples cristae junction security to mitochondrial fusion.

Table of Contents

Abstract ii

Table of Contents iii

List of Figures vi

List of Abbreviations viii

Acknowledgements xii

Chapter 1

Introduction 1

1.1 Mitochondrial Morphology

1.11 Mitochondrial Fusion 2

1.12 Mitochondrial Fission 5

1.13 Mitochondrial Cristae 9

1.2 Functions of Mitochondrial Dynamics

1.21 mtDNA stability 13

1.22 Mitochondrial Quality Control and Mitophagy 14

1.23 Apoptosis 16

1.24 Mitochondrial Trafficking 18

1.3 Mitochondria in Disease

1.31 Mitochondrial Dynamics and the Heart 20

1.32 Cancer and Aging 21

1.33 Diabetes 22

1.34 Neurodegeneration 24

1.4 Screening Mitochondrial Dynamics 25

Chapter 2

Materials and Methods

2.1 Antibodies and Reagents 27

2.2 Imaging Screen 27

2.3 Algorithm Development 28

2.4 Immunoprecipitation, SDS-PAGE and Western Blotting . . . 28

2.5 Electron Microscopy 28

2.6 Oxygen Consumption Assay 29

2.7 Immunofluorescence 29

2.8 ATP measurements 29

2.9 Gel Filtration Chromatography 30

2.10 Cytochrome C release 30

2.11 Condensed Nuclei death assay 30

Chapter 3

Results

3.1 Romo1 is a novel regulator of mitochondrial fusion . . . 31

3.2 Defective cristae and mitochondrial bioenergetics in cells lacking Romo1 37

3.3 Romo1 is REDOX regulated 42

3.4 Romo1 regulates mitochondrial morphology through MINOS and Opa1 46

3.5 Romo1 couples cristae junction closure to mitochondrial fusion 51

Chapter 4

Discussion

4.1 Romo1 is a novel regulator of mitochondrial fusion 55

4.2 Romo1 couples mitochondrial REDOX to mitochondrial morphology 56

4.3 Romo1 as a CJ-checkpoint protein required for mitochondrial fusion 58

4.4 Future Directions 60

4.5 Romo1 and cell death 62

4.6 Concluding Remarks 63

Chapter 5

References 64

Chapter 6

Appendices 78

List of Figures

Figure 1 ROMO1 is a strong candidate in a mitochondrial morphology screen 32

Figure 2 ROMO1 is required for normal mitochondrial morphology . 34

Figure 3 ROMO1 is required for mitochondrial fusion 36

Figure 4 Abnormal cristae in cells lacking Romo1 38

Figure 5 Defective cristae junctions sensitizes cells lacking Romo1 to apoptosis 39

Figure 6 Defective mitochondrial respiration in cells lacking Romo1. 41

Figure 7 Increase in superoxide in cells lacking Romo1 43

Figure 8 Romo1 is REDOX regulated 45

Figure 9 Romo1 interacts with Mitofilin 47

Figure 10 MINOS does not regulate Romo1 activity 49

Figure 11 Romo1 regulates mitochondrial morphology through OPA1 . 50

Figure 12 Romo1 REDOX status couples cristae junction maintenance to mitochondrial fusion 52

Figure 13 Romo1 mediates a cristae junction checkpoint prior to inner membrane fusion 54

Appendix I Mammalian Outer and Inner Mitochondrial Fusion Machinery 78

Appendix II Mammalian Mitochondrial Fission Machinery 79

Appendix III MINOS/MICOS/MitOS complex members and Mammalian Homologues 80

Appendix IV C-terminal tagged Romo1 acts as a dominant negative . . . 81

Appendix V Romo1 mRNA is present in both U20S and GM38 cells and is depleted by RNAi 82

Appendix VI Romo1 REDOX status is regulated by glutathione reductase 83

Appendix VII Cells lacking Romo1 display altered Opa1 processing. 84

Appendix VIII Cells lacking Romo1 display normal expression of the Mitofusins and Drp1 85

Appendix IX Uncoupling between mitochondrial morphology, cytochrome c release, and apoptosis 86

List of Abbreviations

AAA	ATPases Associated with diverse cellular Activities
AD	Alzheimer's Disease
ADP	Adenosine Diphosphate
ALS	Amyotrophic lateral sclerosis
ATP	Adenosine Triphosphate
BAK	Bcl-2 homologous antagonist/killer
BAX	Bcl-2-associated X
BCL	B cell lymphoma
BID	Bcl-2 interacting domain
cAMP	cyclic adenosine monophosphate
CCCP	Carbonyl cyanide *m*-chlorophenyl hydrazine
CHCHD3	Coiled-coil-helix-coiled -coil-helix domain containing 3
CDK1	Cyclin-dependent kinase 1
CMT	Charcot-Marie Tooth Disease
CJ	Cristae Junction
DHE	Dihydroethidium
DRP1	Dynamin-related protein 1
DTT	Dithiothreitol
ER	Endoplasmic Reticulum
ERMES	Endoplamic Reticulum-Mitochondria encounter structure
ERMIONE	ER-mitochondria organizing network
FIS1	Fission 1
FCCP	Carbonylcyanide-4-trifluoromethoxyphenylhydrazone
FCJ1	Formation of Cristae Junctions 1

Fzo	Fuzzy Onion
GDAP1	Ganglioside-induced differentiation-associated protein 1
GFP	Green Fluorescent Protein
GSIS	Glucose-stimulated insulin secretion
GTP	Guanosine Triphosphate
HD	Huntington's Disease
HeLa	Henrietta Lacks
IBM	Inner Boundary Membrane
IM/IMM	Inner Membrane/Inner Mitochondrial Membrane
IMS	Intermembrane Space
LRRK2	Leucine-rich repeat kinase 2
MAPL	Mitochondrial anchored protein ligase
MARCH5	Membrane-associated ring finger (C3HC4) 5
MAVS	Mitochondrial Antiviral Signaling
MDM36	Mitochondrial distribution and morphology 36
MDV1	Mitochondrial division 1
MIB	Mitofusin Binding Protein
MiD49/51	Mitochondrial Dynamics proteins of 49 and 51kDa
MIEF1	Mitochondrial Elongation Factor 1
MFF	Mitochondrial Fission Factor
MFN	Mitofusin
MGM1	Mitochondrial genome maintenance 1
MIA	Mitochondrial intermembrane space assembly
MICOS	Mitochondrial Contact Site
MINOS	Mitochondrial inner membrane organizing system
MIRO	Mitochondrial Rho

MitoPLD	Mitochondrial Phospholipase D
MitOS	Mitochondrial Organizing Structure
MOMA-1	Mitochondrial outer membrane abnormal 1
MOMP	Mitochondrial outer membrane permeabilization
MPP	Mitochondrial Processing Protease
mtDNA	Mitochondrial Deoxyribonucleic Acid
MTGM	Mitochondrial Targeted GxxxG motif
MTP18	Mitochondrial Protein 18kDa
NFκB	Nuclear factor kappa-light-chain-enhancer of activated B cells
NUM1	Nuclear migration 1
OA	Optic Atrophy
OCR	Oxygen Consumption Rate
OM/OMM	Outer Membrane/Outer Mitochondrial Membrane
OMA1	Overlapping with the m-AAA protease 1 homolog
OPA1	Optic Atrophy 1
OXPHOS	Oxidative Phosphorylation
PARL	Presenilin-associated rhomboid-like
PD	Parkinson's Disease
PINK1	PTEN-induced putative kinase 1
PKA	Protein Kinase A
PKC	Protein Kinase C
Rho	Ras homology
RIG-I	Retinoic acid-inducible gene 1
RNAi	Ribonucleic Acid interference
ROMO1	Reactive Oxygen species Modulator 1
ROS	Reactive Oxygen Species

SAM	Sorting and Assembly Machinery
SENP5	SUMO1/sentrin specific protease 5
siRNA	Small interfering ribonucleic acid
SMAC	Second mitochondria-derived activator of caspases
SUMO	Small ubiquitin-like modifier
TOMM20	Translocase of the Outer Mitochondrial Membrane 20
TRAF2/6	TNF receptor associated factor 2/6
U2OS	Osteosarcoma cell line
UBC9	Ubiquitin carrier protein 9
VDAC1	Voltage-dependent anion channel 1

Acknowledgements

The work collected in this document would not be possible without the help of so many people. I'd like to thank my supervisor Dr. Robert Screaton for all his support and guidance throughout this project. Thanks to all members, past and present, of the Screaton lab including: Stephen Baird, Jen Crichton, Chantal Depatie, Qiujiang Du, Ariane Dumoulin, Chandra Eberhard, Myddryn Ellis, Calie Fu, Matt Gaetz, Valerie Lefebvre, Darcey Miller, Edgardo Montes, Mirna Nascimento, Andy Ng, Courtney Reeks, Karine Robitaille, Junichi Sakamaki and Jim Yang. Thanks to our collaborators Heidi McBride, Tim Shutt, Liqun Xu, Miguel Andrade-Navarro and Nancy Mah. Thanks to my thesis advisory committee members Dr. John Bell and Dr. Alex MacKenzie and to my thesis examiners Dr. Mary-Ellen Harper and Dr. Alex MacKenzie for all their dedicated time. Thanks to Lynn Kelly and Kathleen Frost for keeping our facilities running smoothly. Thanks to the University of Ottawa Faculty of Medicine and Department of Cellular and Molecular Medicine for their support and guidance. Thanks to the Children's Hospital of Eastern Ontario and CHEO Research Institute as well our funding agencies the Ontario Institute for Cancer Research and Ontario Graduate Scholarship.

Chapter 1 Introduction

Mitochondria are highly dynamic organelles that act as both regulators and effectors of numerous cellular processes. Early observations identified mitochondria as respiratory units. *Battelli and Stern (1912)* (1) and *Warburg (1913)* (2) both associated cellular respiration with insoluble structures and the central interest in mitochondria became the bioenergetics processes resulting in the production of ATP through metabolic pathways and electron transport. (Reviewed in (3)). This common focus on mitochondria, however, overlooked the diverse role this organelle plays within a cell. Mitochondria are now understood to be critical regulators of cell death pathways including apoptosis, necrosis and autophagy (Reviewed in (4-6)). Mitochondria are also the primary cellular source of reactive oxygen species (ROS) (7), generated by inefficient transport of electrons, predominantly from complexes I and III in the electron transport chain (ETC) (8). While ROS were originally thought of as damaging molecules (Reviewed in (9, 10)), they are now studied in a variety of contexts as important signaling molecules (Reviewed in (8, 11, 12)). Mitochondria have also been shown to play roles in cell signaling independent of ROS. Upon activation, both K-Ras (13) and p53 (14) have been shown to translocate to mitochondria to induce apoptosis and MAVS (Mitochondrial Antiviral Signaling) was identified as an important molecule mediating antiviral signaling responses at the outer mitochondrial membrane (15-18). Furthermore, mitochondria form contacts with the endoplasmic reticulum (ER) through the ER-mitochondria encounter structure

(ERMES) complex and communicate through calcium and phospholipid exchange (Reviewed in (6, 19)). It has been recently demonstrated that ER-contact sites can regulate mitochondrial morphology (20), as well as mitochondrial protein import and mtDNA replication (Reviewed in (19)). Mitochondria play important roles in energy sensing (5, 21), cell cycle regulation (21) and thermoregulation (22). Importantly, these mitochondrial-associated processes are almost all regulated by mitochondrial morphology.

1.1 Mitochondrial Morphology

1.11 Mitochondrial Fusion

Mitochondria exist as a highly dynamic, interconnected network regulated by the opposing processes of mitochondrial fission and fusion, collectively referred to as mitochondrial dynamics. Early microscopy studies on organelle structure and the cell cycle provided the first evidence that mitochondrial morphology is dynamic, as mitochondria fragment prior to cytokinesis and elongate once cell division has occurred (Reviewed in (23)). The processes of mitochondrial fission and fusion are regulated by large GTPases at both the outer and inner mitochondrial membranes (shown in Appendix I). The outer membrane fusion machinery was first identified in a mutant *Fzo Drosophila* strain unable to fuse their mitochondria during spermatogenesis (24). *Fzo* was characterize to be part of a large outer mitochondrial membrane, OMM, complex required for mitochondrial fusion in yeast (25). Two human orthologues to *Fzo* were found to

be responsible for this process in mammals and were termed Mitofusin (Mfn) 1 and 2 (26). Mfn1 and Mfn2 form homo- and/or heterodimers (27) tethering adjacent mitochondria in *trans* through their heptad repeat regions (HR2), mediating the assembly of a dimeric, antiparallel coiled-coil (28). Once tethered, bilayers can initiate mixing of phospholipids through Mitochondrial Phospholipase D (MitoPLD), which is targeted to the OMM and promotes *trans*-mitochondrial membrane adherence by hydrolysis of cardiolipin to phosphatidic acid (29). Phosphatidic acid is thought to either recruit or activate fusion factors or act directly as a fusogenic lipid (30). Although Mitofusin 1 and 2 can functionally compensate for each other to mediate fusion (31), they are also functionally distinct. Mfn1 has higher GTPase activity than Mfn2 (32) and while both knockout models (Mfn1-*null* and Mfn2-*null*) are embryonic lethal, their developments are disrupted in different stages (33). Furthermore, heterotypic *trans* complexes between Mitofusins 1 and 2 have greater fusion efficiency than homotypic *trans* Mitofusion 1 or Mitofusin 2 complexes (34); however, only Mfn2 homotypic complexes are positively regulated by the proapoptotic, Bcl-2 protein, Bax (34). Both Mitofusin 1 and 2 are, however, negatively regulated by the Mitofusin-binding protein, MIB (35).

The inner membrane fusion machinery was first identified as the large inner mitochondrial membrane (IMM) GTPase Mgm1 in yeast (27) and subsequently as Opa1, in mammalian cells (36). The Opa1 gene encodes at least 8 splice variants (37) and in addition to its MPP cleavage site required for

import, Opa1 contains two proteolytic cleavage sites denoted site 1 and 2 (S1 and S2) (38). Consequently, each Opa1 splice variant can produce both a long Opa1 isoform, integrated into the IMM, and one or more short, soluble isoforms, residing in the intermembrane space (39). Both a long and short isoform are required to mediate fusion (40). In the absence of lipids, both long and short monomers are inactive, but upon assembly in a membrane, long isoforms dimerize in *trans*, tethering adjacent inner membranes and allowing assembly of higher order complexes with short isoforms, activating the GTPases of those short isoforms to initiate fusion (41). The proteases that regulate Opa1 processing are poorly understood; however, clear roles are starting to be defined in the literature. Constitutive cleavage of Opa1 at S2 is mediated by intermembrane space AAA (i-AAA) protease, Yme1L, following mitochondrial import (40, 42). Although some constitutive cleavage at S1 is observed, cleavage is primarily induced by loss of inner membrane potential ($\Delta\psi$), experimentally induced by the chemical ionophore carbonyl cyanide *m*-chlorophenyl hydrazine (CCCP) (40, 42). Identifying the protease responsible for S1 cleavage has been arduous, with reports suggesting that the matrix AAA (m-AAA) protease, paraplegin (38), and presenilin-associated rhomboid-like (PARL) protease (43) are involved; although, murine lines lacking paraplegin or PARL display normal Opa1 processing (44). These proteases, along with m-AAA protease complex subunits AFG3L1 and 2 (45), may play indirect or partial roles in regulating S1. Some resolution has been provided, however, by two groups recently identifying

the zinc metalloprotease, OMA1, as the inducible, S1 protease (45, 46), which itself is proteolytically regulated, possibly explaining some of the confounding reports (46).

Coordination of outer and inner membrane fusion is thought to occur through Ugo1, an outer membrane protein essential for mitochondrial fusion in yeast (47). Ugo1 interacts with Fzo1p and Mgm1p, the yeast homologues of Mfns and Opa1, respectively (48), and plays a role in fusion downstream of membrane tethering, presumably involved in lipid mixing (49).

1.12 Mitochondrial Fission

Opposing mitochondrial fusion is the process of mitochondrial fission. The GTPase that regulates mitochondrial fission was first identified in mammalian cells as Drp1 (50) and subsequently in yeast as Dnm1p (51). Drp1 is primarily localized to the cytosol (50), but translocates to the mitochondria to carry out mitochondrial fission (52). Upon recruitment to mitochondria in yeast, Dnm1p self-assembles into oligomeric spirals with a diameter equal to that of mitochondrial constriction sites (53). These spirals undergo conformational changes constricting from an average outer diameter of 120nm to 68nm upon hydrolysis of GTP (54). Several adaptor proteins have been identified as Drp1 recruiting factors. In yeast, Dnm1p is recruited to the OMM by the integral membrane protein Fis1p and its adaptor proteins the WD-repeat containing Mdv1p (55, 56), and the WD40-protein Caf4p (57). Num1p and Mdm36p are also

accessory proteins in yeast that associate with Dnm1p and facilitate the fission process by generating membrane tension through anchoring of mitochondria to actin at the cell cortex (58, 59). Multiple studies in mammalian cells suggested that hFis1 interacted with Drp1 and was responsible for its recruitment to mitochondria in higher eukaryotes (60-62). Overexpression of Fis1, which localizes to the OMM, induced mitochondrial fragmentation (61), while knockdown of Fis1 led to mitochondrial elongation (60). However, conditional HCT166 Fis1$^{-/-}$ cells display normal mitochondrial morphology and rates of mitochondrial fusion (63) and several studies show that Fis1 is not required for association of Drp1 with mitochondria (63-65). Mammalian homologues of yeast accessory proteins Mdv1p and Caf4p have not been identified; however, several groups have recently identified novel proteins involved in Drp1 recruitment and assembly, providing new insight into the mechanisms of mitochondrial fission. *Gandre-Babbe et al. (2008)* identified Mitochondrial Fission Factor (Mff) as a novel OMM-anchored protein involved in mitochondrial fission. They showed that knockdown of Mff induces mitochondrial elongation and Mff and Fis1 exist in separate 200 kDa complexes, suggesting independent roles for the two proteins (66). *Otera et al. (2010)* showed that Drp1 preferentially interacts with Mff over Fis1, and Mff is required for Drp1 recruitment to the OMM and subsequent fission of the mitochondrial network, in a manner independent of Fis1 (63). *Palmer et al. (2011)* identified Mitochondrial Dynamics proteins of 49 and 51 kDa (MiD49 and MiD51, respectively) as novel mediators of mitochondrial fission. MiD49/51 are

OMM-anchored proteins that form foci and rings around mitochondria and promote Drp1 association with mitochondria. Knockdown of these proteins reduce Drp1 recruitment and leads to unopposed mitochondrial fusion and elongation of the mitochondrial network (67). *Zhao et al. (2011)* independently identified MiD51 as Mitochondrial Elongation Factor 1 (MIEF1). They argue for a role of MIEF1 in mitochondrial fusion rather than fission (68). This study is largely based on the observation that overexpression of MIEF1 leads to mitochondrial elongation. The authors attribute the elongation to a role for MIEF1 as an endogenous inhibitor of Drp1 in a model whereby MIEF1 recruitment of Drp1 to mitochondria sequesters it away from functional complexes. *Palmer et al. (2011)*, however, addressed this point by showing that both low and high levels of MiD51/MIEF1 leads to accumulation of Drp1 on the mitochondria; however, only high overexpression leads to elongation, suggesting that the inhibitory role of MiD51/MIEF1 on Drp1 may not be physiological (67). Further studies will be needed to clarify these differing views. The mammalian fission machinery is shown in Appendix II. Other proteins suggested to play a role in mitochondrial fission include MTP18 (69, 70), Ganglioside-induced differentiation-associated protein 1 (GDAP1) (71, 72) and Endophilin B1 (73, 74), whose roles are largely uncharacterized to date.

Mitochondrial fission is highly regulated through post-translational modification of Drp1. Drp1 is regulated by phosphorylation, ubiquitination and SUMOylation. Drp1 is phosphorylated by cAMP-activated PKA at S637 inhibiting

its GTPase activity, resulting in mitochondrial elongation (75). Dephosphorylation at this site is regulated by Ca^{2+}-activated calcineurin, causing Drp1 translocation to the mitochondria (76). During starvation, PKA-mediated phosphorylation and inhibition of Drp1 is important for mitochondrial elongation and protection against autophagy (77). During mitosis, Drp1 is phosphorylated by Cdk1/Cyclin B at S616 promoting mitochondrial fission for distribution to daughter cells (78). This site can also be phosphorylated by PKCδ in post-mitotic neurons where hypertensive encephalomyopathy was associated with increased Drp1/PKCδ interactions and mitochondrial fragmentation (79). The E3-ubiquitin ligases MARCH5 and Parkin have been shown to ubiquitinate Drp1. MARCH5-mediated ubiquitination stabilizes Drp1 on the OMM promoting fission (80, 81) while Parkin-mediated ubiqutination leads to Drp1-degradation by the proteasome (82). Sumoylation is a post-translational modification through the conjugation of a small ubiquitin-like modifier (SUMO). Sumoylation stabilizes Drp1 causing mitochondrial fragmentation and is mediated by Sumo1 (83), Ubc9 (84) and MAPL (85). Sumoylation and stabilization of Drp1 is promoted by Bax and Bak during apoptosis (65). Desumoylation is mediated by the protease SenP5 (86, 87).

Although roles for mitochondrial and cytosolic proteins involved in mitochondrial fission continue to be revealed, a large focus has turned to the role of the endoplasmic reticulum in regulating this process. Important advances were made in this field of study by *Rizzuto et al. (1998)* who showed that close

contacts between ER and mitochondria were important features in Ca^{2+} responses (88), and *de Brito et al. (2008)* who identified ER-associated Mfn2 as an ER-mitochondrial tether, forming homo- or heterotypic complexes with mitochondrial-associated Mfn1 or 2. This tether was shown to be important for mitochondrial uptake of ER-released calcium (89). A recent report by *Friedman et al. (2011)* describes how the ER network crosses over the mitochondrial network at future sites of mitochondrial fission, and are thought to mediate an initial constriction of the mitochondrial network prior to Drp1 recruitment and independent of Drp1, Mff and Mfn2 (20). This dynamic relationship between mitochondria and ER will be important to consider in future studies in the field of mitochondrial dynamics.

1.13 Mitochondrial Cristae

While the gross morphology of mitochondria is defined by the fission and fusion machinery, mitochondria also have a dynamic inner membrane, regulated independently from these processes. The inner membrane is classified into two regions; the portion of the inner membrane adjacent to the OMM, termed the inner boundary membrane (IBM), and membrane invaginations, termed cristae. These two portions of the IMM come together at cristae junctions (CJ) (90). The importance of cristae is thought to be their ability to subcompartmentalize mitochondria. Cristae are the primary site of ATP production (91). They restrict the movement of respiratory chain complexes (91) and limit the diffusion of metabolites such as ADP, a critical metabolite regulating oxidative

phosphorylation (OXPHOS) (*Reviewed in* (92)). Although dynamic redistribution of proteins does occur, cristae are also the principal sites of iron/sulfur cluster biogenesis, protein synthesis and transport of mtDNA-encoded proteins. The IBM is the principal site of proteins involved in mitochondrial fusion and transport of nuclear-encoded proteins (92). These observations highlight the importance of subcompartmentalization of mitochondria and regulation of inner membrane morphology. There are many proteins involved in regulating the structure of the inner membrane. Since one of the primary functions of mitochondrial cristae is to improve efficiency of ATP production, it is not surprising that the ATP synthase, Complex V of the respiratory chain, is involved in regulating cristae morphology (93). Although monomeric ATP synthase is fully capable of ATP synthesis, it has been shown that the complex organizes in dimers (94, 95) and higher oligomers (96), dependent on subunits e and g (Su e/g) (93). While ATP synthase oligomerization correlates with higher efficiency of ATP synthesis (97), this is actually due to the ability of oligomers to generate a force creating curvature of the inner membrane and participate in generating cristae (97). Angular association of two monomers generates a dimer leading to membrane curvature and cristae formation. Furthermore, concentrated localization of ATP synthase dimers at the cristae apex generates a proton sink increasing the proton-motive force contributing to more efficient ATP production (97).

The inner membrane fusion protein, Opa1, is also an important regulator of mitochondrial cristae. Evidence of this was first observed in studies by *Olichon*

et al. (2003) and *Arnoult et al. (2005)* who show that knockdown of Opa1 induces apoptotic cristae remodeling and release of proapoptotic molecules (98, 99). *Frezza et al. (2006)* characterized this association, demonstrating that Opa1 oligomerization between long and short isoforms holds cristae junctions together. These oligomers are disrupted by proapoptotic truncated-Bid (t-Bid), causing opening of CJs and apoptosis (100). Furthermore, this role for Opa1 during cell death was independent from its role in mitochondrial fusion (100).

While the ATP synthase is important in cristae formation and Opa1 in their regulation, maintenance of cristae is obtained by structural components that form a complex at the cristae junctions. The first, and most extensively characterized component is Mitofilin, in mammals, or Formation of Cristae Junctions 1 (Fcj1), in yeast. Mitofilin is an inner membrane protein found to assemble into large multimeric complexes required for the maintenance of cristae junctions (101). The yeast homolog, Fcj1, was identified by similar observations and is proposed to act antagonistically with the ATP synthase to generate mitochondrial cristae (102). As described earlier, ATP synthase oligomerization induces membrane curvature at the cristae apex (97). *Rabl et al. (2009)* show that Fcj1 is enriched at the CJs and overexpression disrupts ATP synthase dimerization suggesting that the spatial distribution and antagonism between Fcj1 and the ATP synthase defines cristae morphology. Where the ATP synthase is enriched over Fcj1, positive membrane curvature generates the cristae tip; conversely, where Fcj1 is enriched over the ATP synthase, synthase oligomerization is inhibited allowing

for negative membrane curvature at the cristae junctions (102). Studies in *C. elegans* support an interaction between the Fcj1 homologues, IMMT1 and 2, and the ATP synthase (103). In mammals, CHCHD3 was identified as a Mitofilin and Opa1 interacting partner, required for maintenance of normal cristae and mitochondrial morphology (104). Knockdown of CHCHD3 results in a loss of Mitofilin and defects in cristae morphology (104). In *C. elegans*, MOMA-1 was identified in an RNAi-screen looking for novel regulators of mitochondrial morphology and was hypothesized to work in the same pathway as CHCHD3 and Mitofilin (105). Knockdown of MOMA-1 leads to defects in cristae morphology (105). Recently, three groups identified very similar complexes in yeast, consisting of Fcj1 and homologues to CHCHD3 and MOMA-1, among others, required for maintenance of CJs, as well as contacts between IM and OM at the inner boundary membrane (106-108). These complexes were termed MITOS/MINOS/MICOS but will be referred to as the Mitochondrial Inner membrane Organizing System (MINOS) since it is the most extensively characterized. MINOS is composed of 6 subunits: Fcj1 (Mitofilin in mammals), Aim5 (Mcs12 in *MICOS)*, Mio10 (Mcs10 in *MICOS,* Mos1 in *MITOS* and recently identified as MINOS1 in mammals (109)) Aim13 (Mcs19 in *MICOS,* CHCHD3 in mammals), Mio27 (Mcs29 in *MICOS*, Mos2 in *MITOS*) and Aim37 (Mcs27 in *MICOS*, MOMA-1 in *C. elegans*) (106-108). Appendix III summarizes these complex members. Fcj1 and Mio10 are the core components of this complex in yeast as *fcj1Δ* and *mio10Δ* strains have more severe growth defects and

destabilization of other complex members. Destabilization of steady state levels of complex members was not observed in the other deletion strains (107). Fcj1 also interacts with the Translocase of the Outer Membrane (TOM) (68) complex and *fcj1Δ* strains have protein import defects through the Mitochondrial Intermembrane space Assembly (MIA) pathway. Destabilization of MINOS in other deletion strains, however, has no defect in protein import; thus, Fcj1/Mitofilin has an additional role in protein import, independent of its role in MINOS in maintenance of CJs (107).

1.2 Functions of Mitochondrial Dynamics

1.21 mtDNA Stability

The cell regulates the morphology of the mitochondrial network in order to carry out a variety of functions. Mitochondrial fusion plays an important role in the stability of mitochondrial DNA (mtDNA). Mitochondrial fusion is important for content mixing, including sharing of mitochondrial lipids, metabolites and mtDNA (110, 111). mtDNA is anchored to the inner membrane (112) and organized in nucleo-protein complexes termed nucleoids, each containing multiple copies of the mitochondrial genome (113) and many associated proteins that differ in mammals and yeast (*Reviewed in* (114, 115)). Due to asymmetrical fission events, mitochondrial content is heterogeneous. This heterogeneity includes mtDNA that differs in sequence and proportions of mutations. This characteristic is called heteroplasmy (116). Although it is thought to be a rare event,

complementation of mutant mtDNA can occur after content mixing, decreasing heteroplasmy and allowing mice with high proportions of mutant mtDNA to retain functional mitochondria (116). The idea that fusion allows for complementation of heteroplasmic mtDNA highlights its importance in mitochondrial inheritance. *Chen et al.* (2005) demonstrate how cells with targeted null mutations in Mfn1 or Mfn2 retain low levels of mitochondrial fusion and the ability to escape mitochondrial dysfunction; however, cells deficient in both Mitofusins or Opa1 are incapable of fusion leading to decreased cell growth, heterogeneous inner membrane potential, decreased respiration (117), and loss of mtDNA nucleoids (110). Together, these data provide evidence for a direct role of mitochondrial fusion in the stability of mtDNA nucleoids.

1.22 Mitochondrial Quality Control and Mitophagy

Autophagy, or “cell eating”, is the generic degradation of cellular material delivered to the lysosome. Primarily thought of as a response to an energy crisis, macroautophagy serves as an adaption to survive during starvation. However, in contrast to this broad definition, autophagy is also capable of being highly selective (*Reviewed in* (118)). One kind of selective autophagy is mitochondrial autophagy, or ‘mitophagy’. Mitophagy encompasses the selective removal of damaged mitochondria and delivery to the lysosome for degradation. Organismal aging is partially attributed to increases in mtDNA mutations (119, 120), increases in ROS (121) and decreases in OXPHOS (122), among changes in other mitochondrial properties. When too much damage accumulates to be

repaired by fusion and content mixing, selective changes in mitochondrial morphology isolate damaged portions of the mitochondrial network and target them for removal by mitophagy. In a damaged portion of reticulum, fission events generate asymmetrical daughter mitochondria: one with high membrane potential and one with low membrane potential. This event leads to an increased probability the healthy mitochondrion will re-fuse with the network and a decreased probability for the unhealthy mitochondrion, due to a decrease in $\Delta\psi$ and OPA1 levels (123). This isolation of damaged mitochondrial fragments generates portions of the network small enough for removal by mitophagy. Loss of $\Delta\psi$ initiates the mitophagy program by inhibiting mitochondrial protein import leading to stabilization and activation of the (PTEN)-induced putative kinase 1, PINK1, which is normally destabilized through its proteolysis following import (124, 125). Ectopic overexpression or CCCP-induced stabilization of PINK1 leads to recruitment of the E3-ubiquitin ligase Parkin to mitochondria (124, 126-128). Genetic studies in *Drosophila* provide support for a PINK1/Parkin pathway *in vivo* (129, 130). Recruitment of Parkin to mitochondria causes K63-linked signaling ubiquitination of a number of targets and recruitment of the LC3-binding protein, p62/SQSTM1 (131, 132). p62 recruits LC3 and targets ubiquitylated cargo into autophagosomes for autophagic degradation (133). Parkin has also been shown to ubiquinate specific targets for proteosomal degradation, such as the Mitofusins (134), and is thought to inhibit fusion of damaged mitochondria with the network. Regulation of mitochondrial morphology is critical for containing damaged

mitochondria and allowing their selective removal through the PINK1/Parkin mitochondrial quality control pathway and degradation by mitophagy.

1.23 Apoptosis

Apoptosis is the process of programmed cell death. Initiated either intrinsically or extrinsically, apoptosis is characterized by cell shrinking and nuclear condensation followed by membrane blebbing and budding of apoptotic bodies consumed by macrophages. Apoptosis has no inflammatory response since the cell never ruptures and is rapidly consumed by phagocytosis preventing secondary necrosis. Engulfing cells do not produce inflammatory cytokines (*Reviewed in* (135)). While all apoptotic cascades converge on the same effector pathway, mitochondria play a more predominant role in the intrinsic initiation pathway. A variety of instrinsic pro-apoptotic signals converge on the mitochondria and initiate mitochondrial outer membrane permeabilization (MOMP). This permeabilization releases pro-apoptotic molecules such as cytochrome C and SMAC/Diablo, among others, into the cytoplasm to activate effector caspases, cysteine proteases that carry out the apoptotic response (*Reviewed in* (136)). MOMP is tightly regulated by the Bcl-2 family of proteins. Bax and Bak are cytosolic, proapoptotic, Bcl-2 family proteins recruited to mitochondria to initiate apoptosis by forming oligomeric pores in the outer mitochondrial membrane. Formation of Bax/Bak pores is regulated by both pro- and anti-apoptotic Bcl-2 proteins (*Reviewed in* (137)). Permeabilization of the OMM is not, however, the only event required to release proapoptotic molecules

into the cytoplasm. Remodeling of mitochondrial morphology is also essential for propagation of apoptotic signaling. Early observations that mitochondrial fragmentation was an event during apoptosis (138, 139) led to further studies suggesting that manipulation of the mitochondrial network can affect sensitivity to cell death (140, 141). Mitochondrial fission is an early event in apoptosis occurring before caspase activation and in a similar time frame to cytochrome C release (140, 142, 143). Although there is conflicting evidence whether mitochondrial fission is required for cytochrome C release (140, 142), or whether they are separable events (143, 144), there is a large body of evidence that regulation of mitochondrial morphology is important in the execution of apoptosis. Upon treatment with an apoptotic stimulus, Drp1 translocates to the OMM (140) and colocalizes with Bax and Mfn2 at scission sites (141). Expression of a dominant negative Drp1 mutant (Drp1K38A) or downregulation of Drp1 by RNAi delays mitochondrial fragmentation, cytochrome c release, caspase activation and cell death (140, 142). Conversely, knockdown of the fusion machinery enhances these processes (142, 145) While the pro-fission molecule, Drp1, was shown to colocalize with Bax upon apoptotic stimuli (140), *Karbowski et al. (2004)* showed, conversely, that mitochondrial fusion was also blocked during apoptosis (146). In contrast, mitochondria hyperfuse during cellular stress to prevent the cell from undergoing apoptosis (147). While the roles of mitochondrial dynamics machinery in apoptosis at the OMM are somewhat unclear, a large focus on IMM dynamics in recent years has provided insight into the regulation of

apoptosis at mitochondrial cristae. As discussed earlier, Opa1 plays an important role in regulating cristae junctions. Opa1 is present as an integral inner membrane protein as well as a soluble intermembrane space protein. These isoforms of Opa1 form higher order oligomers which promote narrowing of cristae junctions and sequestration of cytochrome c (100). These oligomers are disrupted early in apoptosis induced by the addition of proapoptotic tBid, leading to widening of cristae junctions and release of cytochrome c (100). Opa1 processing by presenilin-associated rhomboid-like protease, PARL, is responsible for generating the small pool of IMS Opa1 required for cristae junction maintenance and the prevention of apoptosis (43); however, it is also evident that Opa1 is proteolytically cleaved during apoptosis in response to loss of $\Delta\psi$ and depletion of ATP (148). Regulation of Opa1 processing by the Prohibitins seems to be required for apoptosis as *Phb2*$^{-/-}$ MEFs display defective Opa1 processing and a resistance to apoptosis (149). The proteases directly responsible for apoptosis-induced Opa1 cleavage, however, remain unidentified.

1.24 Mitochondrial Trafficking

Mitochondrial motility and distribution within a cell are important for both organelle function and cell survival. Mitochondrial trafficking is particularly important in polarized cells, such as neurons, in which mitochondria are enriched at sites of high energy demand like synapses, at the distal end of long axonal processes (*Reviewed in* (150)). Mitochondrial motility is also important for mitochondrial segregation during cell division, as mitochondria have to be

separated into individual daughter cells (151). Mitochondria are transported along cytoskeletal tracks and can traffic both away from (anterograde), as well as toward (retrograde) the nucleus using kinesin and dynein motors, respectively (*Reviewed in* (152, 153)). During anterograde transport, mitochondria are tethered to microtubules through a complex with Miro/Milton. Miro1 and 2 are a mitochondrial Rho GTPases tail-anchored to the OMM and contain two GTPase domains and a pair of Ca^{2+}-binding EF-hands (154, 155). The EF-hands serve as Ca^{2+} sensors that allow for Ca^{2+}-induced inhibition of mitochondrial motility (*Reviewed in* (156)). Miros associate with Milton, a cytosolic protein that interacts with kinesin heavy chain (155, 157). Mammalian homologs of the *Drosophila* protein Milton are Grif-1 and OIP106, which associate with kinesin in the absence of a light chain suggesting that Milton might function as an organelle-specific light chain (158, 159). Both Mitofusins interact with Miro/Milton and Mitofusin 2 is required for transport of axonal mitochondria (160). Pink1 also interacts with Miro/Milton and, although its role is unclear, is thought to participate in mitochondrial trafficking (161). Miro has also been associated with regulation of mitochondrial morphology in response to Ca^{2+}. At resting [Ca^{2+}], Miro overexpression promotes fusion; however, at high [Ca^{2+}] Miro overexpression promotes fragmentation (162). These observations suggest that mitochondrial motility mechanisms are integrated with the dynamics machinery and demonstrate another process in which mitochondrial morphology is important.

1.3 Mitochondria in Disease

1.31 Mitochondrial Dynamics and the Heart

Many have observed that in diseased-states mitochondria become abnormally large in heart cells (163-165), implying the capacity for morphological changes to the mitochondrial network in this cell type. Although some have observed an absence of mitochondrial fusion in adult heart cells (166), *Chen et al. (2009)* found that Opa1 protein levels were decreased in both human and rat heart failure leading to a fragmented network and apoptosis. While overexpression of Opa1 tubulated the network, it failed to rescue the cell death (167). *Ashrafian et al. (2010)* found that a C452F mutation in Drp1 is associated with an inherited dilated cardiomyopathy in the mouse model called Python. While homozygous mutations are embryonic lethal, the heterozygous mutation leads mitochondrial elongation and cardiac ATP depletion, hypothesized to contribute to this cardiomyopathy (168). Interestingly, *Ong et al. (2010)* showed that upon ischemia/reperfusion injury, cardiac mitochondria undergo Drp1-dependent fragmentation leading to cell death. This fragmentation could be reverted by overexpression of Mfn1 or 2 or with Drp1K38A (dominant-negative), leading to decreased MOMP and reduced cell death. These effects could be reproduced using the Drp1-inhibitor, mitochondrial division inhibitor-1 (mdivi-1), suggesting the potential for this chemical to be used as a cardioprotective pharmalogical therapeutic (169). It is interesting that *Ong et al. (2010)* found elongation to be protective in cardiac injury while *Ashrafian et al. (2010)* found

elongation to be metabolically damaging and potentially causative of a cardiomyopathy. These report suggest the potential for inhibition of mitochondrial fission to be protective in short term injury models but damaging in the long term and provide insight into the role of mitochondria in heart disease.

1.32 Cancer and Aging

The ability of a cancer cell to evade apoptosis is a classic *Hanahan and Weinberg (2000)* “hallmark of cancer” (170) and evidence from over a decade of research has implicated the mitochondria in the regulation of all the classical hallmarks of transformation; including, apoptosis, disabled autophagy, sustained angiogenesis and limitless replicative potential, among others (171). Cancer cells also display a shift from mitochondrial respiration to aerobic glycolysis known as the "Warburg effect” (172). These observations are indicative of changes in mitochondrial biology in tumorigenesis and make mitochondria a promising target for therapeutics. Modulation of the Bcl-2 protein family, metabolic inhibition, and ROS regulation are some of the strategies, among others, being tested as mitochondrial-targeted chemotherapeutics (173).

Changes in mitochondrial structure and function are also associated with aging. Mitochondrial elongation has been commonly observed in aging cells and is associated with loss of cristae and a decrease in ATP production (174-176). Furthermore, multiple studies have observed a decrease in Fis1 and Drp1, and an increase in Mfn1, during senescence, accompanied mitochondrial elongation,

a decrease in mitochondrial function and an increase in mitochondrial damage (81, 177-179). Interestingly, it is also hypothesized that a decrease in fission and fusion cycles is associated with age in order to decrease mitochondrial flux and damage, thus improving quality control (180).

1.33 Diabetes

Hyperglycemia following feeding is counteracted by secretion of insulin from the pancreatic beta cells, which stimulates glucose uptake into peripheral tissues. Insulin secretion from the beta cells is stimulated when glucose is metabolized through glycolysis and OXPHOS by mitochondria. This leads to an increase in the ATP/ADP ratio, inhibition of ATP-sensitive K^+ channels on the plasma membrane, membrane depolarization and opening of Ca^{2+} channels. Ca^{2+} influx causes the release of insulin granules packaged in vesicles into the bloodstream, through exocytosis (*Reviewed in* (181, 182)). Islets from type 2 diabetic patients exhibit impaired glucose-stimulated insulin secretion (GSIS) and display a number of mitochondrial dysfunctions including reduced mitochondrial membrane potential, decrease ATP production and high density of swollen mitochondria (183). Under apoptosis-inducing high glucose and fatty acid concentrations, mimicking diabetic conditions, beta cell mitochondria fragment due to a decrease in fusion and GSIS is subsequently reduced. Blocking fragmentation by knockdown of Fis1 rescues these defects (184). Interestingly, *Park et al. (2008)* showed that while overexpression of Fis1 fragmented beta cell mitochondrial networks and overexpression of Mfn1 elongated these networks,

both manipulations led to decreased mitochondrial ATP content and impaired GSIS. Expression of a dominant-negative Mfn1, however, caused fragmentation but had no effect on OXPHOS or GSIS, indicating that the absolute status of the mitochondria does not determine beta cell function but rather the mitochondrial dynamics machinery can play a role in coupling mitochondrial metabolism to insulin secretion (185). These observations as well as those of *Ashrafian et al. (2010) (168)* in the heart, suggest that rather than mitochondrial morphology being a determinant for function it is the dynamic and adaptive nature of the mitochondrial network that imparts its resilience to cellular stresses. Elongation of the mitochondrial network is generally thought to be prosurvival and enhance functionality of mitochondrial programs; however, in these contexts inhibiting mitochondrial fusion led to a decrease in ATP content and reduced the functionality of both beta cells and cardiac cells, contradicting the generic hypothesis that mitochondrial fusion is a protective mechanism that is metabolically advantageous (77, 110, 117, 147, 169, 186, 187). It is possible that this uncoupling comes from a short-term benefit of inhibiting fission that becomes detrimental in the long term. Stronger evidence for the role of dynamics proteins in GSIS comes from *Zhang et al. (2011)* who generated a beta-cell specific knockout of Opa1, which led to impaired glucose-stimulated ATP production and insulin secretion (188). Taken together, these data implicate mitochondrial dynamics in the coupling of glucose metabolism to insulin secretion and provide insight to the role of mitochondria in diabetes.

1.34 Neurodegeneration

Mitochondrial function is closely linked to neurodegeneration in numerous disease models. 188 genetic loci have been associated with adult-onset neurodegenerative diseases including Alzheimer's Disease (AD), amyotrophic lateral sclerosis (ALS), Charcot-Marie-Tooth disease (CMT), Huntington's Disease (HD), Parkinson's Disease (PD), and optic atrophy, among others (189). Of 106 identified genes, at least 36 (34%) have an association to mitochondria either directly (24 genes), or indirectly (12 genes) (189). The strongest links between neurodegeneration and mitochondrial dynamics are that mutations in MFN2 (190), and GDAP1 (71) cause CMT neuropathies type 2a and 4a, respectively, while mutations in OPA1 cause dominant optic atrophy (191, 192). Many other mitochondrial defects in neurodegeneration are related to mitochondrial transport and morphology. AD is associated with defective trafficking of mitochondria and fragmentation. Overproduction of pathogenic amyloid-β leads to downregulation of Opa1 and Drp1 and an upregulation of Fis1. Drp1 reconstitution rescues mitochondrial distribution, while reconstitution of Opa1 rescues mitochondrial morphology (193, 194). In PD, the PINK1/Parkin mitophagy pathway is intimately linked to mitochondrial dynamics; however, there are discrepancies as to how relevant this pathway is in a physiological context (195). Mitochondrial dynamics is also implicated in PD, however, in other contexts. Upon overexpression of pathogenic α-synuclein, the predominant protein found to aggregate and form Lewy Bodies in the substantia nigra of PD

patients, neuronal mitochondrial networks fragment and mitochondrial trafficking is slowed, likely through reductions in levels of Mfn1 and 2 (196). The PD-associated gene leucine-rich repeat kinase-2 (LRRK2) disrupts the dynamics of both the microtubule (197) and mitochondrial networks (198). LRRK2 interacts with Drp1 and promotes mitochondrial fragmentation, likely through an increase in the levels of Drp1 (198). PD-associated mutations in the protein DJ-1/PARK7 also leads to mitochondrial fragmentation (199). In HD, mitochondrial morphology is altered by an increase in Drp1-dependent fission and Opa1-dependent cristae remodeling (200). In HD patient lines, Drp1 is upregulated while Mfn1 is downregulated (201). Pathogenic mutant Huntington protein binds Drp1 and induces mitochondrial fragmentation (202). These data, among others, suggest a broad and important role for mitochondrial dynamics in neurodegenerative diseases.

1.4 Screening Mitochondrial Dynamics

Given the emerging importance of mitochondrial dynamics in various physiological contexts, we sought to identify novel regulators of mitochondrial morphology through an unbiased genome-wide RNAi screen. Identifying novel regulators may also identify potential therapeutic targets for diseases in which mitochondrial morphology is altered. Using this approach we identified Reactive Oxygen Species Modulator 1 (ROMO1) as a novel regulator of mitochondrial fusion and cristae integrity.

Romo1 is a small protein of approximately 8.9kDa characterized as a membrane bound protein localized to mitochondria with a predicted single transmembrane domain (203, 204). Romo1 was originally identified as a protein upregulated in head and neck patient tumor samples after developing resistance to 5-FU (204, 205). This effect of Romo1 upregulation is attributed to the hypothesis that Romo1 promotes ROS production (204), allowing for the compensatory upregulation of anti-oxidant proteins which confer an adaptive responsive and resistance to 5-FU treatment (205).

This role of Romo1 as a positive regulator of ROS is thought to be required for cell proliferation through ERK (Extracellular signal-regulated kinase) activation (206) and suppression of $p27^{Kip1}$ (207). Furthermore, Romo1 is shown to mediate a feedback loop during proliferation via the expression and degradation of Myc (208). Promotion of ROS production by Romo1 has also been shown to be required for serum-deprivation induced apoptosis (209) and mechanistically Romo1 has been shown to recruit TNF complex II and Bcl-x_L to the mitochondria in response to TNFα, whereby Bcl-x_L promotes the reduction of mitochondrial membrane potential, leading to increased ROS and apoptosis (210). The role of Romo1 in regulation of ROS, proliferation and apoptosis, as well as its newly described contribution to tumor cell invasiveness (211), suggests Romo1 may play an important role in tumorigenesis and may have important therapeutic implications.

Chapter 2 Materials and Methods

2.1 Antibodies and Reagents

TOMM20 (Santa Cruz, 1:2000), F1B, Core 2 and Cox1 (all from Mitosciences, 1:1000), FLAG M2 (Sigma, 1:2000), Mitofilin (Abcam, 1:500), CHCHD3 (Abcam, 1:1000), VDAC1 (Cell Signaling, 1:1000), Opa1 (BD Transduction Labs, 1:1000), Opa1 (Abcam, 1:1000), Cytochrome C (BD Pharmingen, 1:1000), AIF (Santa Cruz, 1:1000). GSR (Abcam, 1:2000). Txn2 (Abcam, 1:1000), Mfn1 (Abcam, 1:500), Mfn2 (Abnova, 1:1000), Drp1 (BD Bioscience, 1:1000) Lipofectamine RNAiMAX, Hoechst and Mitotracker Red were all from Invitrogen. CCCP, Antimycin A, N-Acetylcysteine, Sepharose 4B, and Etoposide were all from Sigma. Oligomycin and FCCP were from Seahorse Bioscience. Caspase inhibitor QVD was from Calbiochem.

2.2 Imaging Screen

Pools of four siRNA SMARTpool duplexes targeting 18,255 human genes (Dharmacon) were spotted into 384 well plates. 10 nM of siRNA was reverse transfected into 450 HeLa cells (P34-36) using 0.025 uL of Lipofectamine RNAiMAX (Invitrogen). 72 hr after transfection, cells were fixed and stained with anti-TOMM20 antibody and 1 ug/mL Hoechst 33342 to visualize mitochondria and cell nuclei, respectively. 8 fields per well were acquired using an automatic Cellomics Vti microscope equipped with a 40X objective. Robust Z-scores were calculated as [x – median(sample)]/[median absolute deviation X 1.4826].

2.3 Algorithm Development

After algorithm analysis, images from 10 wells of the elongation and fragmentation end were manually inspected to verify an elongated and fragmented state.

2.4 Immunoprecipitation, SDS-PAGE and Western Blotting

5 ug of plasmid DNA was transfected into a 10cm plate of HEK293T cells using 10 ug PEI (SIGMA). 40 h later cells were collected in PBS, pelleted and lysed in 1 mL ice-cold Co-IP buffer (25 mM Tris pH 7.5, 150 mM NaCl, 50 mM NaF, 0.5 mM EDTA pH 8, 0.5% TX-100, 5 mM β-glycerophosphate, 5% glycerol and 1 mM DTT and 1 mM PMSF). Lysates were then sonicated and centrifuged at 13 000 rpm for 20 min. 10 uL of Anti-FLAG M2 Beads (SIGMA) were washed with cold Co-IP buffer and incubated with samples on a rotary shaker at 4°C overnight. Beads were rinsed with Co-IP buffer, Co-IP buffer with 1M NaCl, then water prior to elution with Laemmli sample buffer for SDS-PAGE. Western blotting with the indicated antibodies was performed in 5% milk in TBS + 0.1% Tween-20, and signals were revealed using ECL (Amersham).

2.5 Electron microscopy

In a 6-well dish, 125 000 cells were reverse transfected with siRNA for 72 hr, washed with PBS, pelleted and resuspended in 2% glutaraldehyde/PBS for embedding.

2.6 Oxygen consumption assay

Cells were reverse transfected on Seahorse XF24 cell culture microplate on day 0. Where applicable, 4 hr after transfection lentivirus was added to wells. Culture medium was changed to a total volume of 500 uL on day 1. On day 3, cells were washed 3X with 500 uL of Seahorse XF assay medium and a mito stress test was performed using oligomycin, FCCP and Antimycin A (all at 0.5 uM). Cell lysates were collected and protein quantified using BCA (Thermo Scientific) for normalization of oxygen consumption rates.

2.7 Immunofluorescence

Cells seeded in 384-well imaging plates were fixed in 3.7% formaldehyde and 5ug/mL Hoechst. After 15min, cells were washed once with glycine/PBS and then permeabilized with 0.1% Trition X-100. Cells were washed once with PBS and blocked in 3% BSA/PBS prior to staining with antibodies. Plates were imaged on an Olympus Fluoview FV1000 Confocal Laser Scanning Biological Microscope.

2.8 ATP measurements

72h after siRNA transfection cellular ATP content was measured using CellTiter-Glo Luminescent Cell Viability Assay (Promega). Luminescence was read on a BioTek Synergy2 plate reader and normalized to cell number.

2.9 Gel Filtration chromatography

72 hr after siRNA transfection, cells were washed once with PBS and scraped into 500 uL CoIP Buffer without DTT. Samples were sonicated for 10 sec and centrifuged at 13 000 rpm for 20 min. Supernatants were applied to Sepharose 4B column and 250 uL fractions were collected every 8 min for SDS-PAGE and Western Blotting analysis.

2.10 Cytochrome C release

Cells were reverse transfected with siRNA as described above and 72 hr later infected with Adenovirus expressing a TET-inducible tBid (gift from G. Shore, McGill University) in the presence of 1ug/mL doxycycline and 12.5 uM QVD. Cells were fixed and stained with cytochrome C and TOMM20 antibodies, imaged using the Cellomics Arrayscan VTi. Cytochrome C release from TOMM20-positive structures was quantified using a colocalization algorithm.

2.11 Condensed nuclei cell death assay

Cells were reverse transfected with siRNA as described above and 72 hr later treated with etoposide for 20 hr. Cells were then fixed in 3.7% formaldehyde, stained with 10 ug/mL Hoechst, and imaged using an OPERA confocal imager (Perkin Elmer). Condensed nuclei were quantified using an algorithm based on nuclear size and intensity of Hoechst staining.

Chapter 3 Results

3.1 Romo1 is a novel regulator of mitochondrial fusion

To identify novel regulators of mitochondrial morphology, we conducted a genome-wide RNAi screen evaluating the function of 18255 genes in the genome with respect to mitochondrial morphology. The screen was carried out using siRNA pools containing 4 duplexes targeting each of the 18255 genes arrayed into 384-well screening plates in triplicate. 72h after reverse transfection of siRNA pools, HeLa cells were fixed and stained by either immunofluorescence targeting the OMM protein Tomm20, or with the potentiometric mitochondrial dye MitoTracker Red^{TM} (Figure 1A). The internal controls for the screen were individual siRNA duplexes targeting the fission and fusion machinery, Drp1 and Mfn1/2, resulting in an extreme elongation or fragmentation phenotype, respectively (Figure 1B, top). To unbiasedly score mitochondrial morphology after the RNAi-screen, an algorithm was developed using Cellomics vHCS Scan image analysis software quantifying the length to width ratio (L:W) of the mitochondrial network, herein referred to as Aspect Ratio. This algorithm neglects any perinuclear staining (Figure 1B, bottom, orange), which is difficult to classify as fragmented or elongated, and averages the remaining mitochondrial stain (Figure 1B, bottom, blue) under each condition across 10 fields in triplicate. The algorithm accurately and reproducibly separates morphological differences between the internal controls siCON, siMfn1/2 and siDrp1 (Figure 1C). The raw

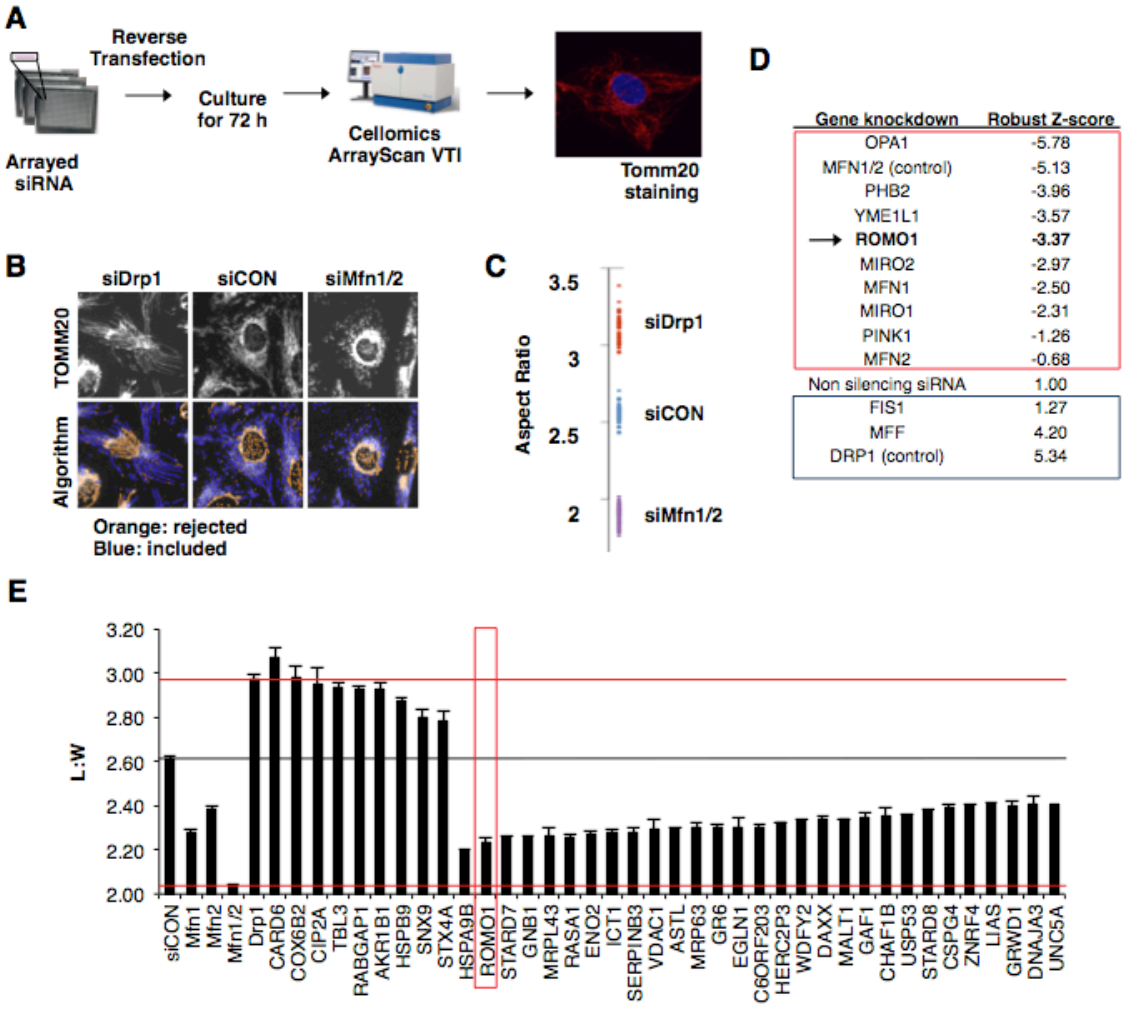

Figure 1 ROMO1 is a strong candidate in mitochondrial morphology screen. A. The high throughput mitochondrial morphology assay. Hela cells in 384 well plates were fixed 72 h after transfection and stained with TOMM20 antibody and Hoechst to monitor the status of the mitochondrial network and nuclei, respectively. Fluorescence images (40X magnification) were acquired using an automated Cellomics Vti microtiter plate microscope. B. Representative images of stained HeLa cells that display control, fused, or fragmented phenotypes marked with key algorithm features. The Cellomics vHCS Scan Morphology algorithm was applied to the network measuring the Aspect ratio Equivalent to Ellipse metric of the individual mitochondrial fibers. The algorithm uses TOMM20 staining (in blue) but negates anything perinuclear (orange) and measures the length:width (aspect) ratio of each segment of the network and averages all of the measurements across multiple fields to quantify the mitochondrial morphology in a population basis. C. Scatter plot of Length:Width (aspect) ratio as determined by the algorithm shows robust separation of cells with control, fused (DRP1 siRNA), and fragmented (MFN1/2 siRNA) mitochondria. D. Table showing the Robust Z-score of ROMO1 and known regulators of mitochondrial dynamics in the RNAi screen. The Robust Z-score is the distance of the value from the median in standard deviation units. E. Aspect ratio of top gene candidates found in morphology screen. Most robust siRNA duplex from the deconvoluted pool of 4 is shown.

screening values were consistent between replicates with a mean Pearson correlation coefficient pairwise comparison of the 3 datasets equal to 0.82. The screen yielded many hits that are known to regulate mitochondrial morphology including OPA1, YME1L1, MFN1 and MFF, among others listed in Figure 1D. Novel candidate genes identified in the primary screen were validated by deconvoluting the siRNA pools into individual siRNA duplexes and assessing the effect on mitochondrial morphology in Figure 1E. Among this list of candidate genes was Romo1 (highlighted). Romo1 knockdown causes dramatic mitochondrial fragmentation (Figure 2A) with 3 out of 4 of the individual siRNA duplexes (Figures 2B), identifying Romo1 as the top candidate novel regulator of mitochondrial morphology. Romo1 was identified by *Chung et al. (2006)* as a positive regulator of reactive oxygen species (204), involved in cellular proliferation (206-208), senescence (212), apoptosis (209, 210, 213), and in tumorigenesis (211). *Zhao et al. (2009)* identified Romo1 independently as Mitochondrial Targeting GxxxG Motif (MTGM), a single pass transmembrane protein of the inner membrane and a positive regulator of mitochondrial fission (203), an interpretation that conflicts with our observation that Romo1 knockdown causes mitochondrial fragmentation. A significant concern when using RNA interference is the potential for off-target effects (214); a concern that is amplified in a genome-wide RNAi screen. In order to properly validate a candidate gene we use genetic rescue. Wobble nucleotides in the Romo1 cDNA seed region complementary to siRNA duplex 3 were mutated to generate an siRNA-resistant

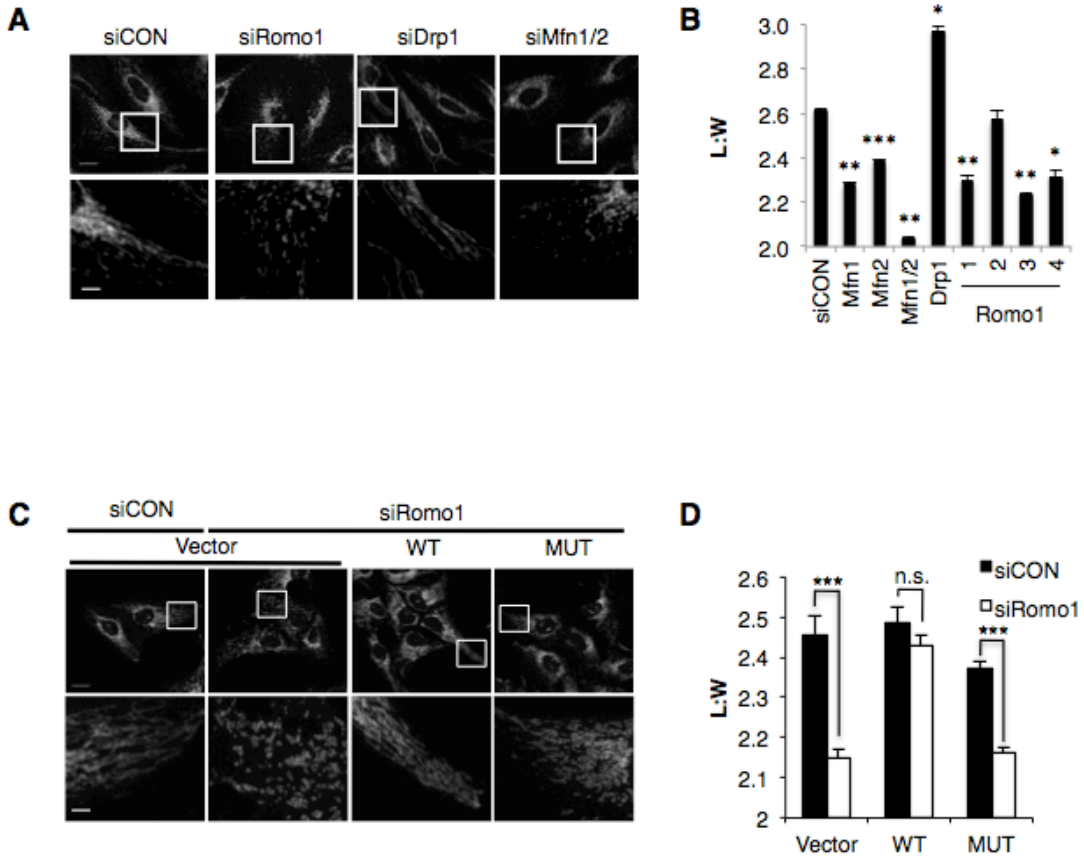

Figure 2 ROMO1 is required for normal mitochondrial morphology A. Photomicrographs of HeLa cells transfected with the indicated siRNAs. Scale bar = 20 nm. Inset shown at bottom, scale bar = 5 nm. B. Histogram showing quantitation of aspect ratio for deconvoluted set of ROMO1 siRNAs shown in A. Effect of knockdown of MFN1/2 and DRP1 controls is shown. * $p < 0.05$. ** $p < 0.01$. *** $p < 0.001$. C. Rescue of ROMO1 knockdown phenotype in U20S cells with siRNA-resistant ROMO1 wt cDNA Effect of ROMO1 non-functional FFAA mutant is shown. D. Histogram showing the aspect ratio for control cells and cells expresing siRNA-resistant wt and FFAA constructs in ROMO1 knockdown cells shown in E. * $p < 0.05$. ** $p < 0.01$. *** $p < 0.001$

rescue construct. As a negative control we generated a nonfunctional mutant, mutating two highly conserved, C-terminal, phenylalanine (Phe 67 and Phe 70) residues, hypothesized to mediate a functional interaction, to alanines from an siRNA-resistant cDNA template. This hypothesis stems from the observation that tagging Romo1 at the C-terminus generates a dominant-negative gene product, shown in Appendix II, suggesting Romo1 functionality lies in its C-terminus. This dominant-negative effect of a Romo1 C-terminal tag likely underlies the discrepancy in Romo1 function between our report and that of *Zhao et al. (2009)* who used overexpression of Romo1-v5 as a primary reagent. In Figure 2C, micrographs demonstrate that in the presence of an empty vector control, Romo1 knockdown causes fragmentation. This can be rescued by expression of the siRNA-resistant wild-type Romo1 but not by the siRNA-resistant mutant Romo1-FFAA, identifying Romo1 as a bona fide regulator of mitochondrial morphology. These results are quantified in Figure 2D. A bimolecular complementation *in vitro* fusion assay depicted in Figure 3A (215) shows that cells lacking Romo1 have about 50% less mitochondrial fusion than controls cells (Figure 3B). This suggests that Romo1 is required mitochondrial fusion, rather than an inhibitor of fission. The residual fusion activity, however, is sufficient for normal mitochondrial morphology if opposing mitochondrial fission is completely blocked by expression of a dominant-negative Drp1 (Drp1K/E), shown in Figure 3C and 3D.

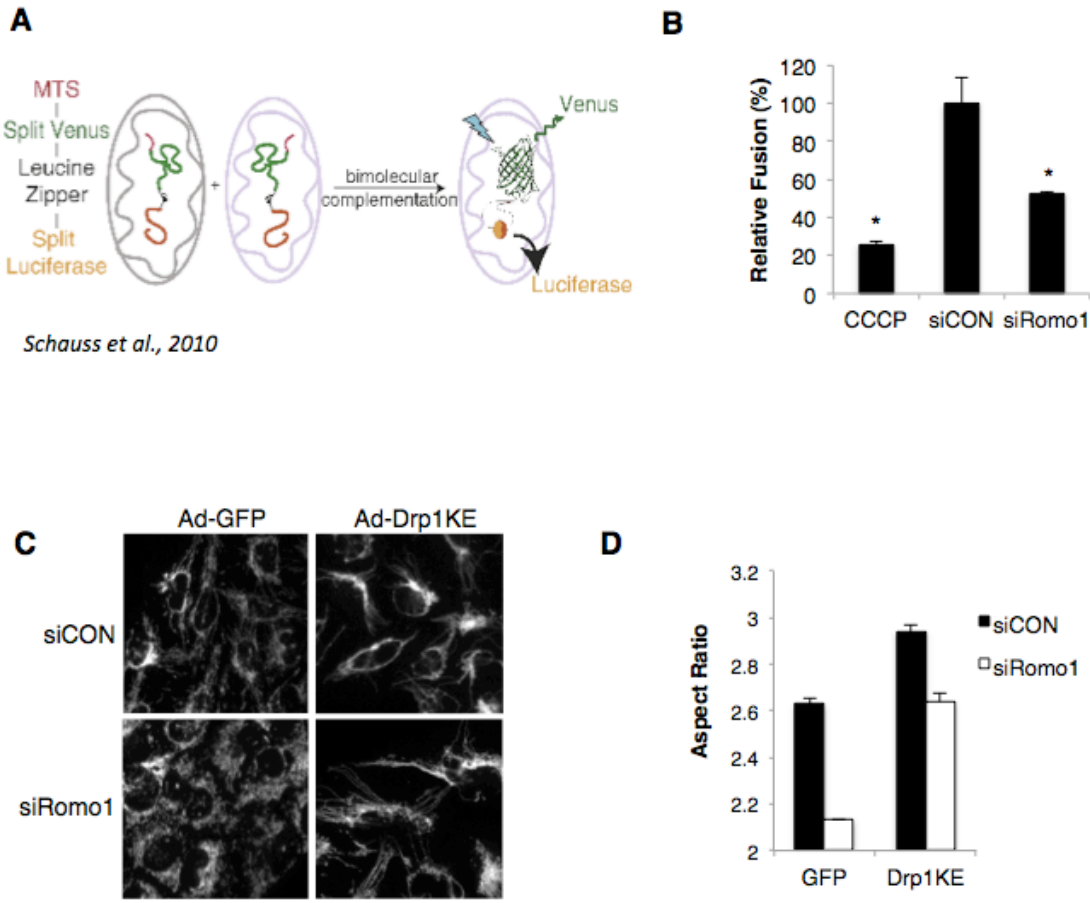

Figure 3 ROMO1 is required for mitochondrial fusion. A. Depiction of an in vitro fusion assay using bimolecular complementation of a split-venus and split-luciferase. B. In vitro fusion assay showing luciferase values generated using mitochondria from control or ROMO1 siRNA transfected cells* $p < 0.05$. C. Micrographs showing Tomm20 staining of mitochondrial morphology in DrpKE rescue of Romo1 knockdown cells. D. Histogram showing restoration of normal aspect ratio in ROMO1 knockdown cells expressing dominant negative Drp1 (Drp1K/E).

3.2 Defective cristae and mitochondrial bioenergetics in cells lacking Romo1

Using electron microscopy we analyzed mitochondrial ultrastructure in Romo1-depleted cells. While normal mitochondria have discernible cristae, mitochondria in cells lacking Romo1 are either devoid of cristae or have defects in cristae junctions resulting in the formation of cristae stacks (Figure 4A). Despite these changes to cristae morphology, Romo1 knockdown cells display normal levels of mitochondrial marker proteins (Figure 4B). Defects in cristae morphology are quantified in Figure 4C. Cells lacking Romo1 have less than 50% of the mitochondrial cristae in control cells normalized to either number of mitochondria or mitochondrial length. Furthermore, Romo1-depleted cells have a significant population of mitochondria with cristae that are detached from the inner membrane and are completely closed with no CJs (arrow in 4B); a phenotype very rarely observed in control cells. To further evaluate the defects in cristae we looked at cytochrome C release in response to pro-apoptotic tBid (Figure 5A and 5B). 8hr after infection with Adeno-tBid, U2OS cells release 20% of the cytochrome C normally sequestered in mitochondrial cristae. Fragmentation of the mitochondrial network by RNAi targeting Mitofusin 1 and 2, either alone or together, results in a sensitization to cytochrome C release as previously seen (140, 142). Conversely, blocking mitochondrial fission by Drp1 knockdown results in protection against tBid-induced cytochrome C release. As expected from ultrastructural analysis, knockdown of Romo1 sensitizes U20S cells to tBid-induced cytochrome C release.

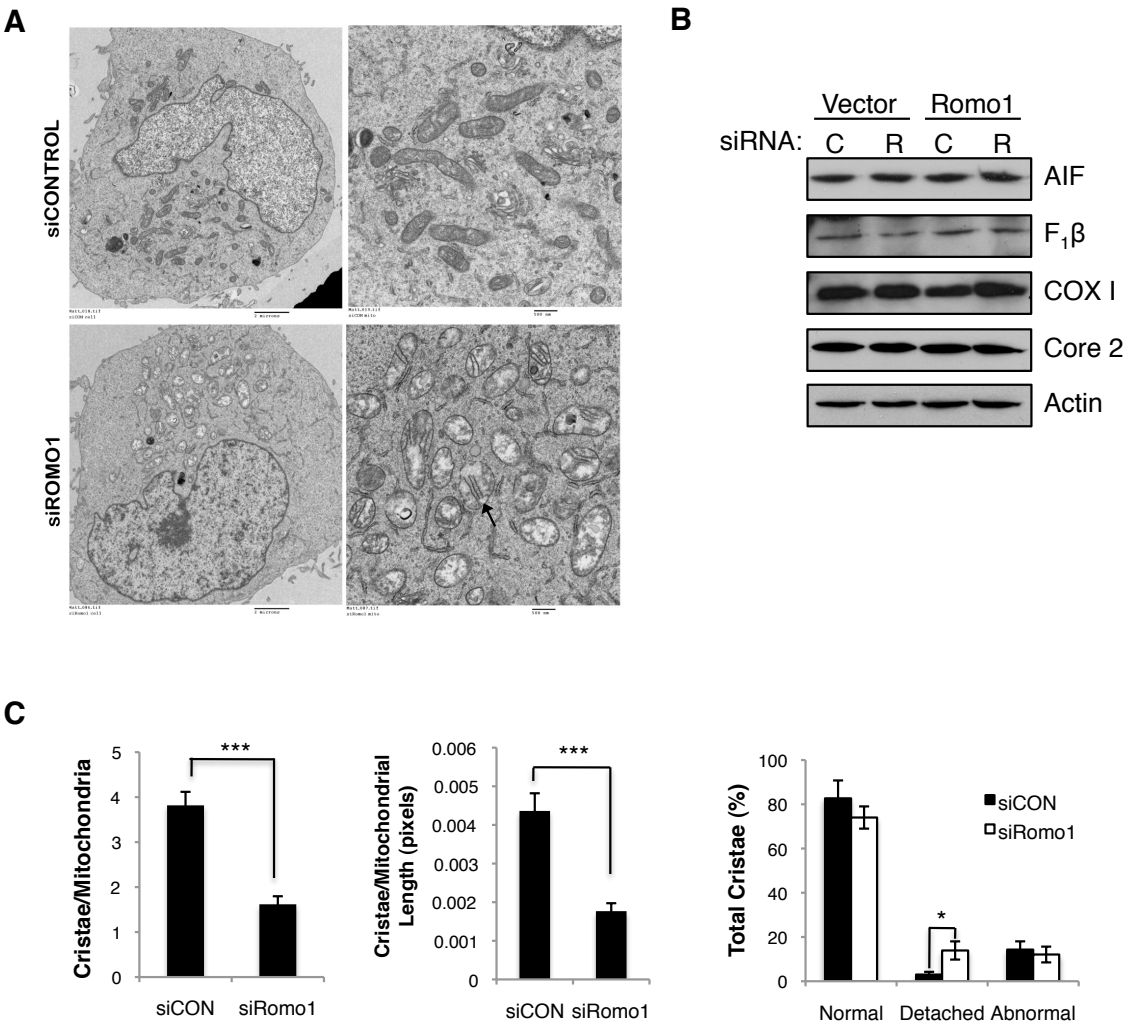

Figure 4 Abnormal cristae in cells lacking ROMO1. A. Electron micrographs of control or ROMO1 knockdown U2OS cells that highlight relative electron paucity and altered cristae in cells lacking ROMO1. Magnification = 1500X (left) and 4000X (13). Arrow indicates cristae stacks. B. Western blot for mitochondrial markers AIF, ATP synthase F1 B1 subunit, COX1, CORE2. Actin loading control is shown. C. Histograms showing number of cristae per unit length of mitochondria in pixels in U2OS cells transfected with control or ROMO1 siRNA, (*** $p < 2.1e\text{-}6$); the number of cristae per mitochondrion in U2OS cells transfected with control or ROMO1 siRNA, (*** $p < 3.7e\text{-}6$); and the percentage of U2OS cells with cristae with normal, detached or abnormal appearance transfection with control or ROMO1 siRNA (* $p < 0.05$)

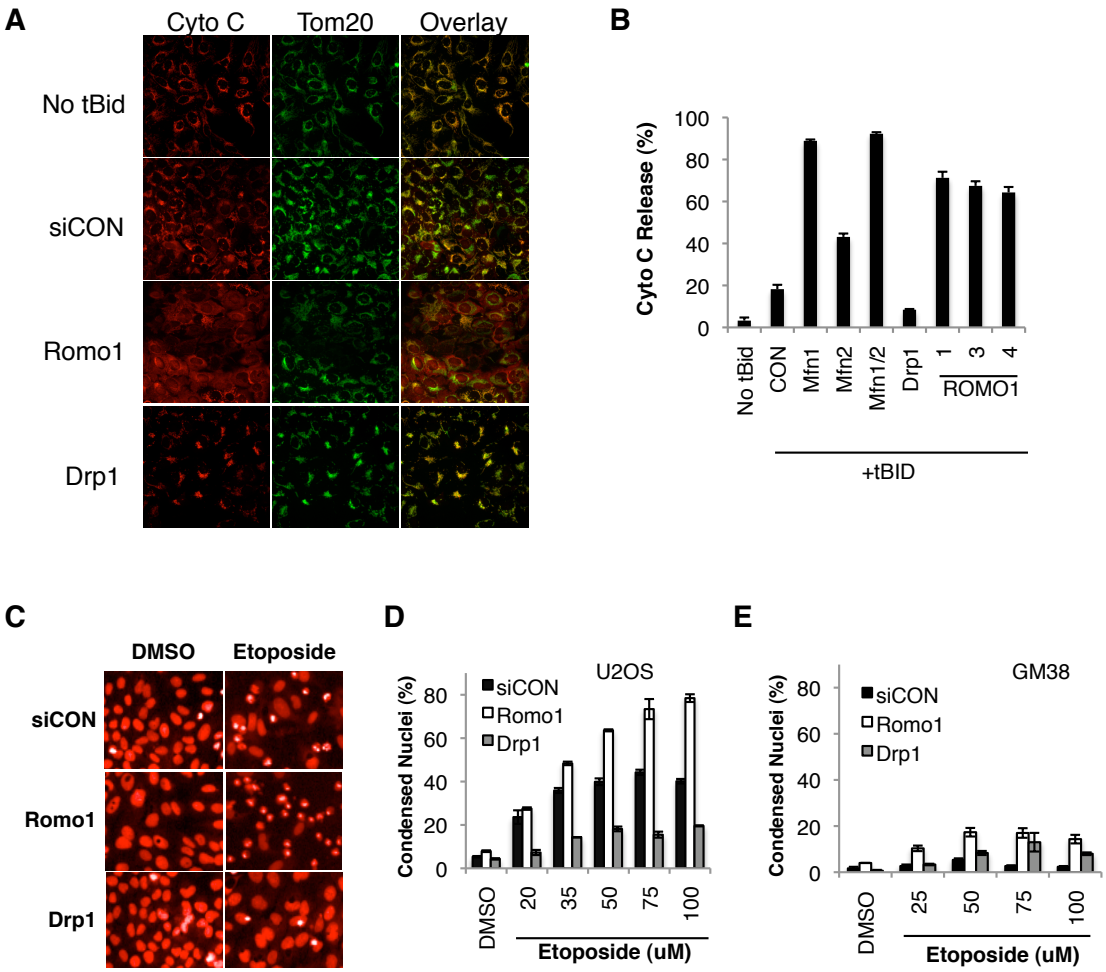

Figure 5 Defective cristae junctions sensitizes cells lacking Romo1 to apoptosis. A. Photomicrographs showing effect of ROMO1 knockdown on cytochrome C release in response to 8hr infection with Adeno-tBid. B. Histogram showing effect of ROMO1 knockdown with three independent siRNAs on cytochrome C release depicted in A. Effect of knockdown of DRP1 and MFN1/2 alone or together is shown. C. Photomicrographs showing effect of ROMO1 knockdown on apoptosis by condensed, apoptotic nuclear morphology in response to 20hr treatment with 75uM etoposide D. Histograms showing effect of increasing dose of etoposide on apoptosis as quantified by condensed, apoptotic nuclear morphology in control (black bars), ROMO1 (white bars), or DRP1 (gray bars) knockdown U2OS cells. E. Histogram showing effect of gene knockdown on apoptosis, as in D, in GM38 normal human fibroblasts.

Using etoposide as an apoptotic stimulus, we observe that Romo1 knockdown also sensitizes U2OS cells to downstream cell death as measured by condensed, apoptotic nuclear morphology seen in Figure 5C and quantified in 5D. Interestingly, Romo1 knockdown does not sensitize GM38 cells, normal human fibroblasts, to etoposide-induced apoptosis (Figure 5E) indicating a potential therapeutic window in targeting the mitochondrial fusion in cancer. Furthermore, Romo1 is upregulated in 14.2% of colorectal cancers (www.cbioportal.org) suggesting a role for Romo1 in transformation as observed elsewhere (211). Importantly, Romo1 mRNA is expressed in both U2OS and GM38 cells (Appendix IIIA) and Romo1 siRNA nearly completely abrogates mRNA levels (Appendix IIIB), as detected by qPCR. Since mitochondrial cristae are functionally associated with mitochondrial metabolism, we assessed mitochondrial bioenergetics in cells lacking Romo1. Romo1 knockdown did not significantly alter ATP content in either glycolytic or oxidative U2OS cells, while the cytotoxic agent etoposide depleted cells of ATP (Figure 6A). Cells lacking Romo1 also displayed normal mitochondrial membrane potential as indicated through positive staining by the potentiometric dye MitoTracker Red, while the addition of the uncoupler CCCP depleted cells of $\Delta\psi$ (Figure 6B). Oxidative phosphorylation of mitochondria in cells lacking Romo1 was assessed measuring oxygen consumption rates (OCR) over the course of a Mito Stress Test. Surprisingly, Figure 6C shows that basal OCR of cells lacking Romo1 is similar to that of control cells. Treatment with the ATP synthase inhibitor, oligomycin,

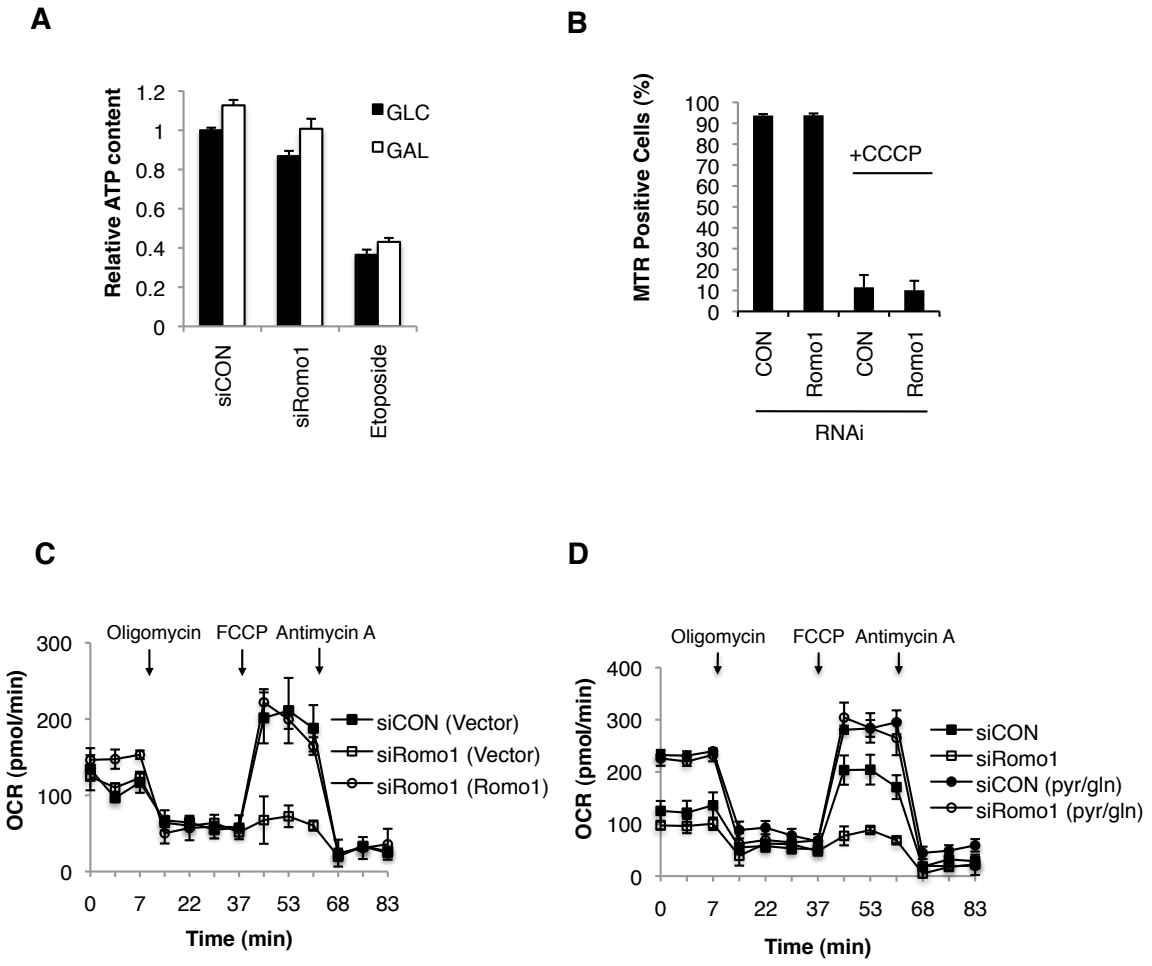

Figure 6 Defective oxygen consumption in cells lacking Romo1. A. ATP levels in glycolytic (left) and oxidative (13) U2OS cells transfected with siRNA targeting ROMO1, DRP1, and MFN1/2. The effect of cytotoxic agent etoposide is shown as control. B. Mitotracker Red staining reveals mitochondrial inner membrane potential in control and ROMO1 knockdown cells. Effect of CCCP treatment is shown. C. Oxygen consumption in control or ROMO1 knockdown cells under basal conditions or following oligomycin, FCCP, and Antimycin A treatment (all at 0.5 uM) is shown. D. Oxygen consumption in control or ROMO1 knockdown cells in presence or absence of pyruvate and glutamine (pyr/gln). Timing of treatment with oligoymcin, FCCP, and Antimycin A is shown.

increases $\Delta\psi$ leading to inhibition of electron transport and a decrease in OCR, termed state 4 respiration, which is also unchanged in Romo1-depleted cells. Treatment with the uncoupler, carbonylcyanide-4-trifluoromethoxyphenylhydrazone (FCCP), leads to uncoupled maximal respiration. Under these conditions, control cells reach an OCR higher than basal; however, cells lacking Romo1 fail to respond to FCCP, suggesting an impaired ability to maximally respire. This defect can be genetically rescued with expression of an siRNA-resistant Romo1 cDNA. Treatment with the complex III inhibitor Antimycin A inhibits electron transport and OCR in both control and Romo1 knockdown cells. Interestingly, in Figure 6D, supplementation of the Mito Stress Test assay medium with pyruvate and glutamine rescues the state 3 defect observed in Romo1-depleted cells, suggesting that these cells deplete their fuel sources more quickly than control cells or have less reducing equivalents available as substrates for electron transport. Taken together, these results identify a defect in cristae integrity in cells lacking Romo1 leading to a sensitization to apoptotic stimuli and a defect in oxidative phosphorylation.

3.3 Romo1 is REDOX regulated

Given that much of the literature on Romo1 is based on its role in regulating ROS production, we looked at superoxide levels in the absence of Romo1. In Figure 7, we show that cells lacking Romo1 have an approximate 2-fold upregulation in superoxide production as measure by dihydroethidium (DHE)

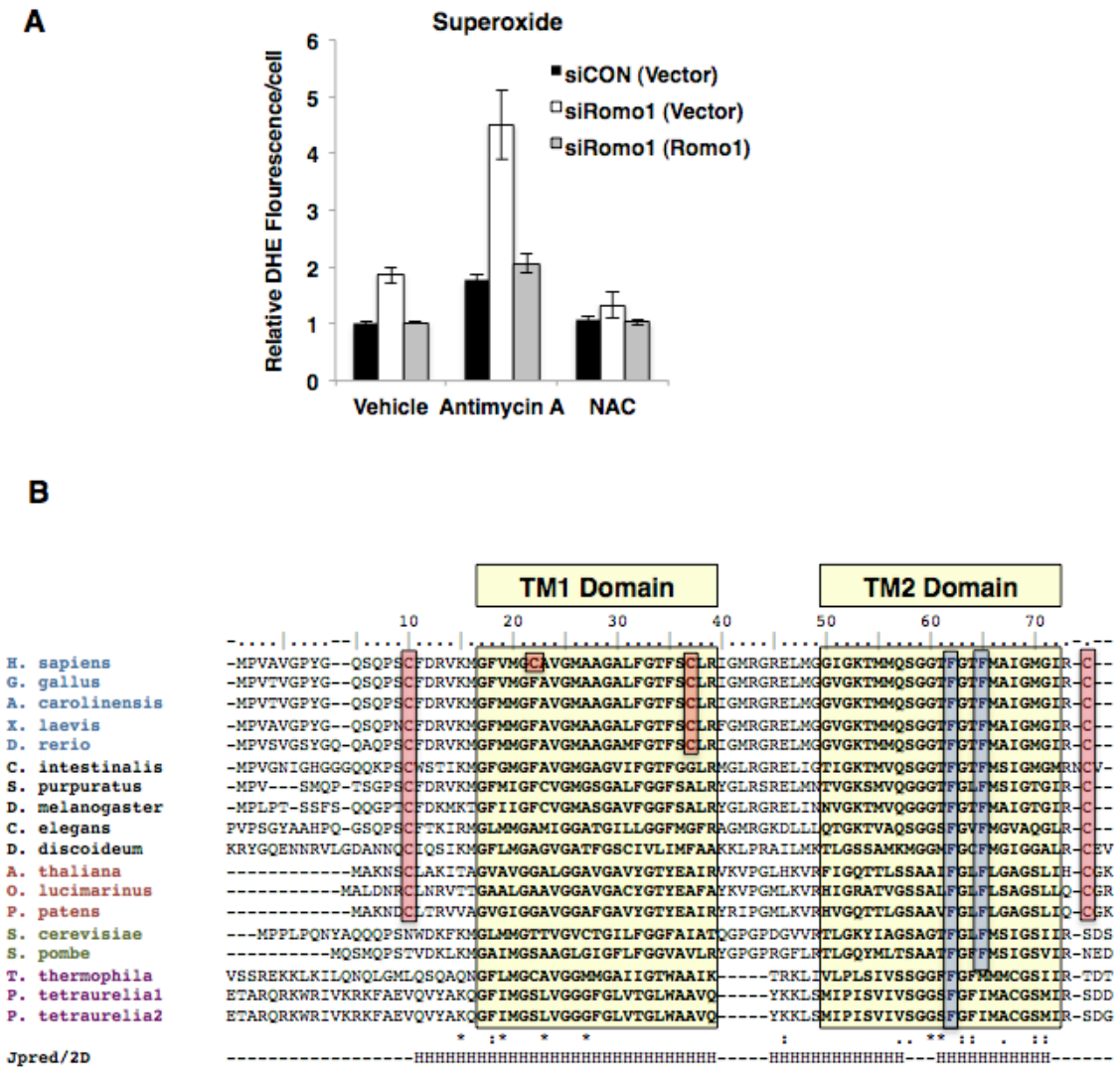

Figure 7 Increase in superoxide in cells lacking Romo1. A. Dihydroethidium (DHE) fluorescence emitted from cells transfected with control or ROMO1 siRNA with or without siRNA-resistant ROMO1. Effect of treatment with complex II inhibitor Antimycin A and N-acetyl cysteine (NAC) is shown. B. Alignment of ROMO1 amino acid sequence in eukaryotes. Conserved Cys residues, putative transmembrane sequence and C-terminal domain indicated.

staining. Addition of Antimycin A to controls cells gives a 2-fold upregulation of superoxide relative to the vehicle control. Romo1 knockdown and treatment with Antimycin A leads to a synergistic increase in superoxide, approximately 4.5 fold higher than untreated control cells and 2.5 fold higher than control cells treated with Antimycin A. Treatment with the ROS scavenger N-acetyl-cysteine (NAC) inhibits the upregulation of superoxide seen in Romo1 knockdown cells. We hypothesized that Romo1 may couple ROS signaling to mitochondrial morphology and generated an alignment of the Romo1 protein sequence in Figure 7B to look for possible REDOX-regulated domains. We found four cysteine residues (highlighted in red), two of which are highly conserved, but interestingly not found in *S. pombe* nor *S. cerevisiae* strains of yeast. These cysteines are found in the N-terminal domain and at the extreme C-terminus. We found two putative transmembrane domains that would place these Cys residues adjacent to one another and provide structural potential for REDOX regulation. We hypothesized these cysteine residues may form REDOX-regulated disulfide bridges as found in a number of other proteins (*Reviewed in* (216)). In Figure 8A, we found that exogenous FLAG-Romo1 generates a single species at ~10kDa on a standard denaturing SDS-PAGE (in the presence of DTT). However, FLAG-Romo1 lysates run on a non-reducing SDS-PAGE (in the absence of DTT) produce a species at ~10kDa, another at ~20kDa and then a laddering of species up to > 245kDa. Interestingly, the non-functional Romo1 mutant, FFAA, has more

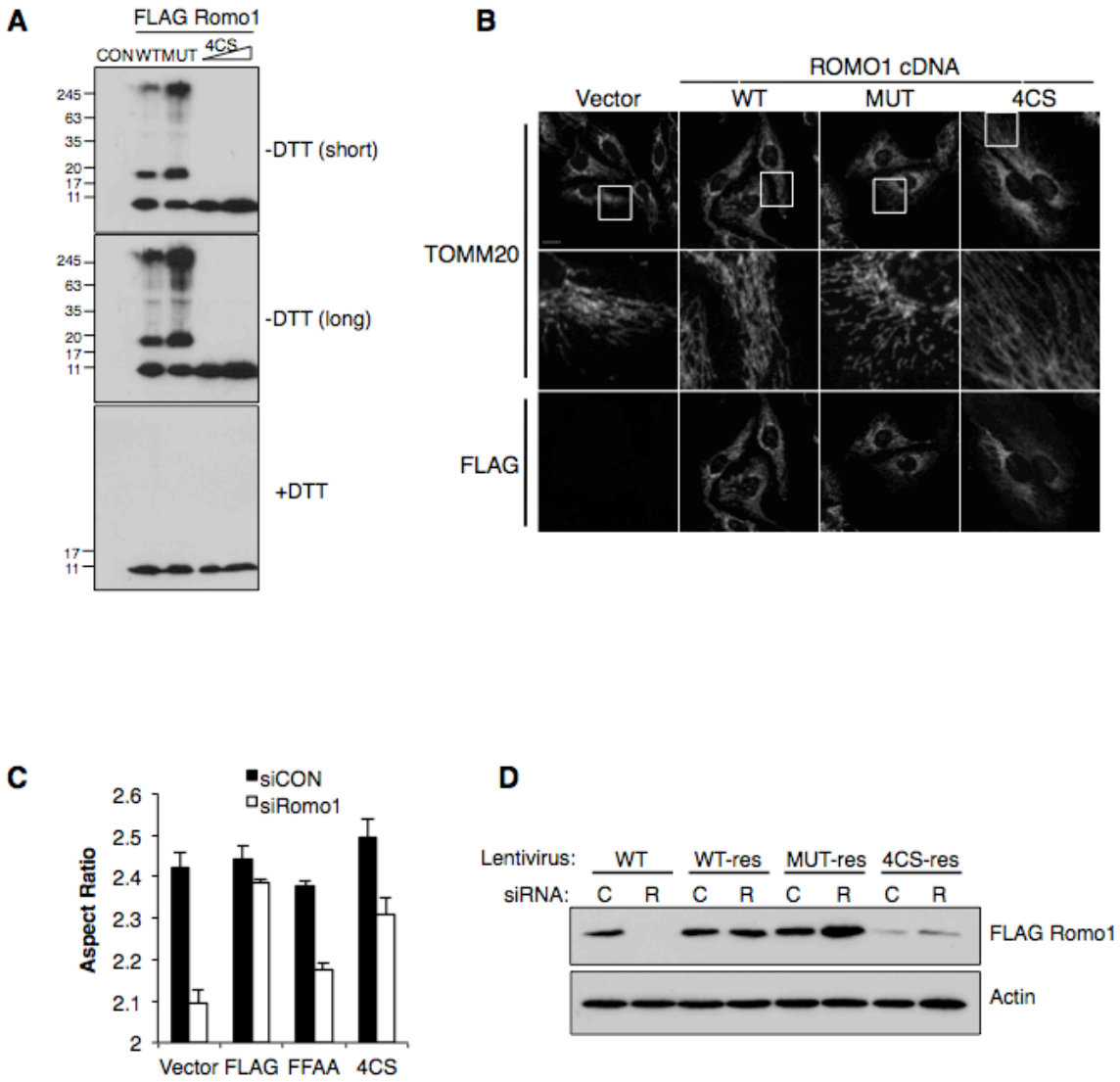

Figure 8 Romo1 is redox regulated. A. Western blot of FLAG tagged ROMO1 WT, ROMO1-FFAA, and ROMO1-4CS following resolution on reducing (+DTT) and non-reducing (-DTT) gels. Short and long exposures of the non-reducing gel blot are shown. B. Fluorescence micrographs showing TOMM20 staining in U2OS expressing siRNA resistant FLAG-ROMO1 wt, -MUT, or -4CS constructs. C. Quantitation of mitochondrial aspect ratio is shown in B. D. Western blot of Romo1 WT and siRNA resistant FLAG-ROMO1 wt, -FFAA (119) and ROMO1-4CS in U2OS cells transfected with control (C) or ROMO1 (R) siRNA probe with anti-FLAG antibody. Actin loading control is shown.

of the oxidized higher molecular weight (HMW) species. However, mutating all 4 cysteine residues found in Romo1 (Figure 7B) to serines generates a mutant (named 4CS) that is constitutively reduced. Functional analysis of these mutants by overexpression and staining of the mitochondrial network reveals that while wild-type FLAG-Romo1 overexpression does not change mitochondrial morphology, overexpression of the FFAA mutant causes mild fragmentation and overexpression of FLAG-Romo1-4CS mutant causes elongation of the mitochondrial network (Figure 8B). These data are quantified in Figure 8C and a western blot in Figure 8D reveals that this elongation causes by FLAG-Romo1-4CS occurs at very low expression relative to the other constructs. Importantly, knockdown of glutathione reductase, a mitochondrial REDOX enzyme, enhances oxidation of Romo1, supporting the hypothesis that Romo1 activity is regulated by mitochondrial REDOX within the cell. Knockdown of thioredoxin 2, however, had no effect (Appendix IV).

3.4 Romo1 regulates mitochondrial morphology through MINOS and Opa1

The yeast homologue of Romo1, Mgr2, has recently been characterized as an accessory protein to the structural complex MINOS, which is responsible for CJ maintenance (106, 107). Mgr2 has also been characterized as a regulator of the presequence translocase, involved in protein import (217). Given the defects in cristae integrity we observed in cells lacking Romo1, we asked if Romo1 interacts with Mitofilin, the core member of MINOS in mammals. Figure 9A shows that Mitofilin co-immunoprecipitates with Romo1 WT, MUT and 4CS.

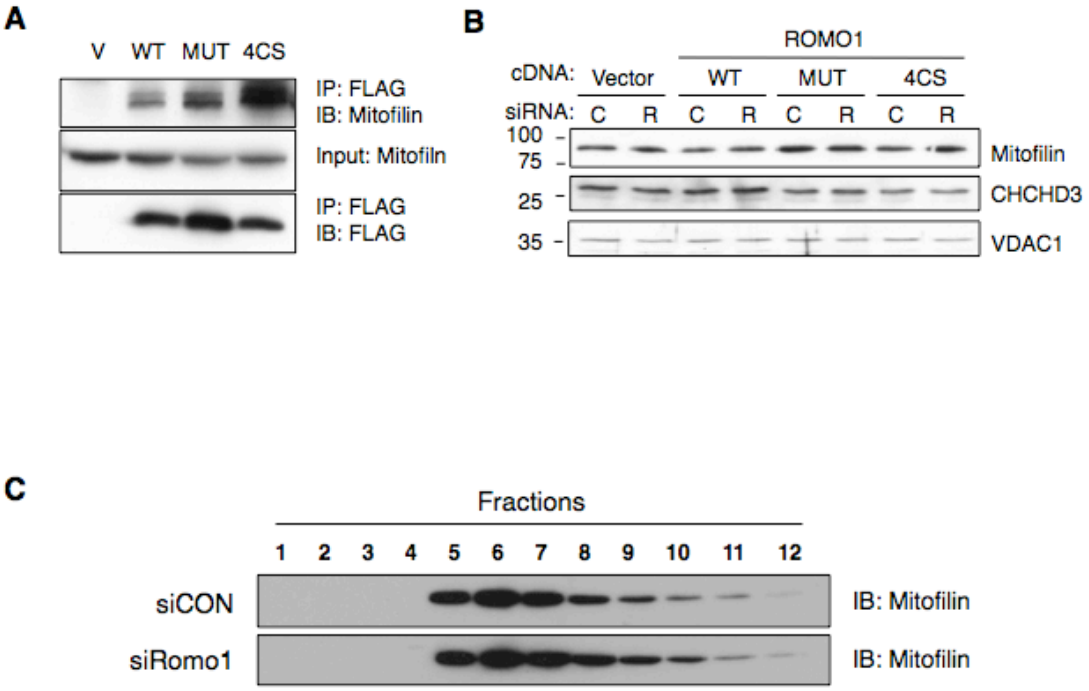

Figure 9 Romo1 interacts with Mitofilin. A. Co-immunoprecipitation of the MINOS complex protein mitofilin with FLAG-ROMO1. Complex formation with ROMO1-FFAA (119) and ROMO1-4CS also shown. B. Western blot of mitofilin and CHCHD3 in control and ROMO1 knockdown cells. Effect of expression of si-Resis-ROMO1 wt, -FFAA, and -CA mutants is shown. VDAC immunoblot shown as loading control. C. Western blot analysis of mitofilin in size fractionated extracts from control, ROMO1 knockdown cells.

Mitofilin interacts with the constitutively active 4CS-mutant approximately 2 to 3-fold more strongly. To reveal the functional consequence of this interaction we looked at protein levels of Mitofilin and CHCHD3, another member of mammalian MINOS. Figure 9B shows that the protein levels of these MINOS members are unchanged in cells lacking Romo1 or expressing Romo1 mutant cDNAs. Figure 9C shows that in cells lacking Romo1, Mitofilin complex size was also unchanged, as evaluated by gel filtration chromatography, as it eluted in similar fractions to control cells. Since Romo1 does not seem to affect Mitofilin protein or complex stability, we asked if MINOS regulates Romo1. Figure 10A and B show that knockdown of MINOS members, Mitofilin and CHCHD3, did not effect Romo1 protein levels or REDOX status, respectively.

To further evaluate the functional relationship of the interaction between Romo1 and Mitofilin we looked at mitochondrial morphology in the absence of MINOS. If Romo1 and MINOS act in a genetic pathway regulating mitochondrial fusion, knockdown of MINOS members should phenocopy knockdown of Romo1. Surprisingly, in Figure 11A, we found that knockdown of Mitofilin caused mitochondrial elongation to a similar extent as that of Drp1 knockdown. Since knockdown of Romo1 and Mitofilin cause different phenotypes with respect to mitochondrial morphology, we evaluated their effect on the inner membrane fusion GTPase, Opa1. Interestingly, Romo1 knockdown causes an imbalance in Opa1 isoforms leading to an overabundance in band C and less band D, relative to control (Figure 11B). Mitofilin knockdown leads to an accumulation of band C

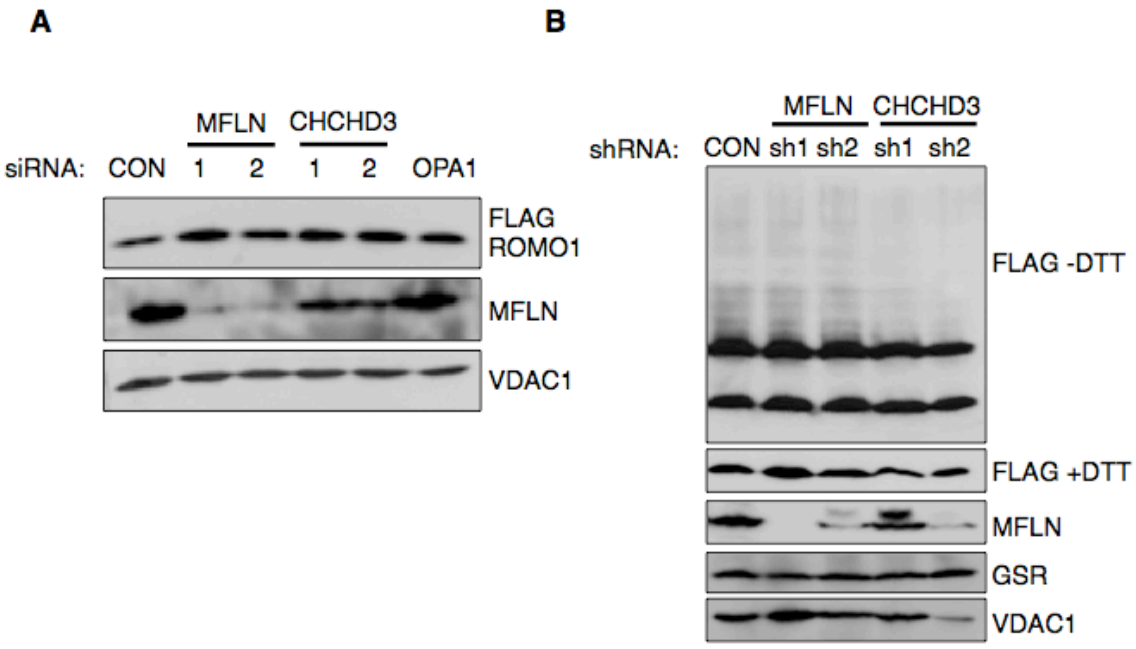

Figure 10 MINOS does not regulate Romo1 activity A. Western blot showing levels of FLAG Romo1 in stably expressing FLAG Romo1 U20S cells in siCON, siMFLN and siCHCHD3 transfected cells. Western blot was also probed for levels of Mitofilin (MFLN) and VDAC1 as controls. B. Western blot of FLAG tagged ROMO1 WT following resolution on reducing (+DTT) and non-reducing (-DTT) gels, 96h after infection with lentivirus encoding shRNAs against CON, Mitofilin (MFLN) and CHCHD3. Western blot was also probed for Mitofilin, GSR and VDAC1 as controls.

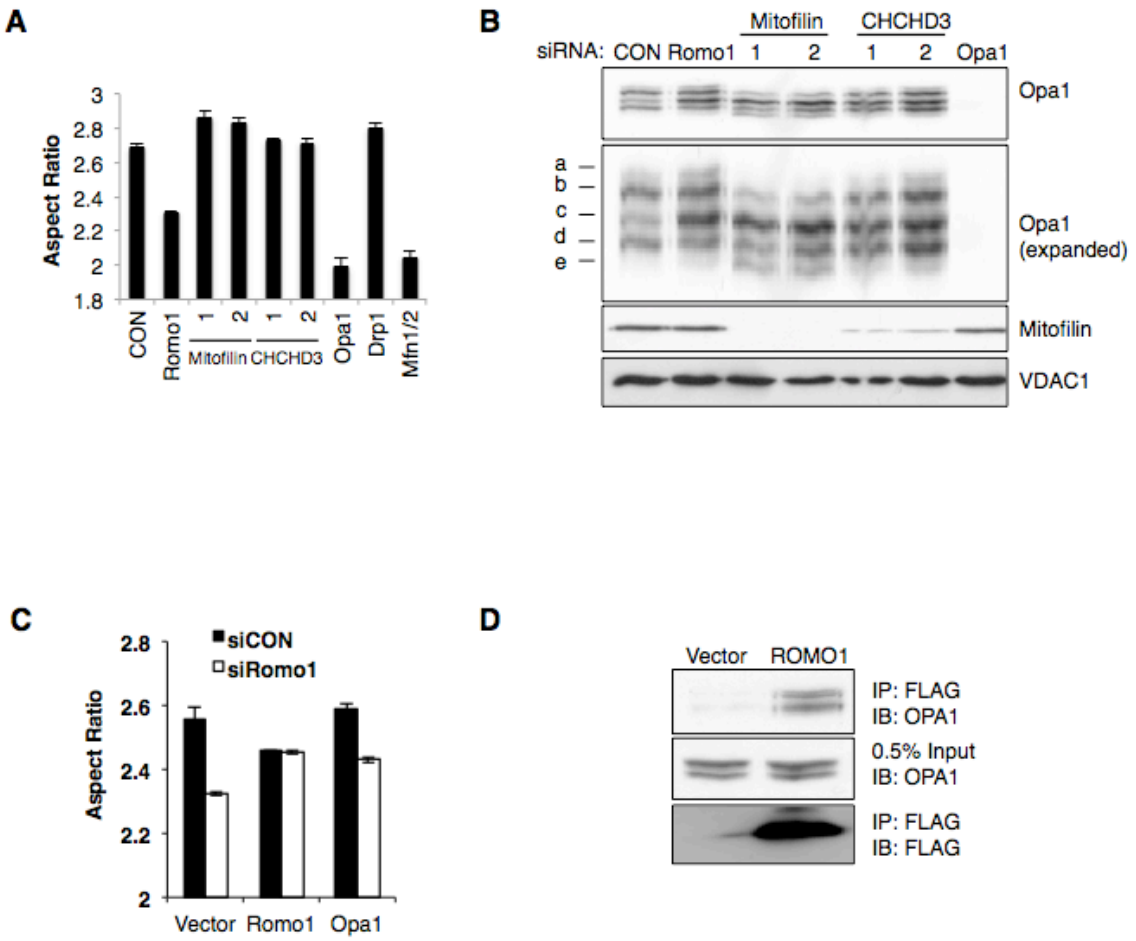

Figure 11 Romo1 regulates mitochondrial morphology through Opa1 A. Histogram showing the network aspect ratio in Mitofilin or CHCHD3 knockdown cells. Effect of knockdown of ROMO1, OPA-1, Drp1, and Mfn1/2 is shown. B. Western blot showing relative abundance of OPA1 isoforms in control, ROMO1, Mitofilin, CHCHD3, and OPA1 knockdown cells. The vertical axis of the bottom OPA1 blot was expanded for ease of visualization of the specific OPA1 isoforms. Western blots for Mitofilin and VDAC loading are shown. C. Histogram showing effect of overexpression of OPA1 isoform v1 partially restores the reduction in aspect ratio in ROMO1 knockdown cells. Rescue with siRNA-resistant ROMO1 wt is shown. D. Western blot of FLAG-Romo1 immunoprecipitation. Co-immunoprecipitation of OPA1 is shown. 0.5% input of OPA1 is shown as a control.

and alternatively a processing of band A to band E. Knockdown of CHCHD3 induces a subtle increase in band C. These data suggest that Romo1 and MINOS act upstream of Opa1 in regulation of cristae and mitochondrial dynamics, although they likely act in a nonlinear pathway. These results are supported by a partial restoration of normal mitochondrial morphology in cells lacking Romo1 by overexpression of Opa1v1 (Figure 11C). Appendix V shows that the defect in Opa1 processing in Romo1-depleted cells can be genetically rescued with Romo1 WT and 4CS cDNAs but not with the FFAA mutant, which causes an accumulation of band b rather than c. Knockdown of Romo1 does not cause any changes in Mfn1, Mfn2 nor Drp1 (Appendix VI). Since Romo1 is required for normal OPA1 isoform balance, we asked if OPA1 also forms a complex with Romo1. Figure 11D shows that OPA1 also co-immunoprecipiates with FLAG-Romo1, supporting the idea that Romo1 regulates mitochondrial morphology through OPA1.

3.5 Romo1 couples cristae junction closure to mitochondrial fusion

In order to elucidate a model to explain how Romo1 regulates mitochondrial fusion and cristae integrity, we used Romo1 mutants to evaluate their ability to compensate for loss of either Mitofilin or OPA1 with respect to mitochondrial dynamics and maintenance of cristae junctions. In Figure 12A, we observe that overexpression of neither Romo1, inactive Romo1-FFAA, nor constitutively active Romo1-4CS was able to revert the phenotypes caused by knockdown of Mitofilin or OPA1 with respect to mitochondrial dynamics,

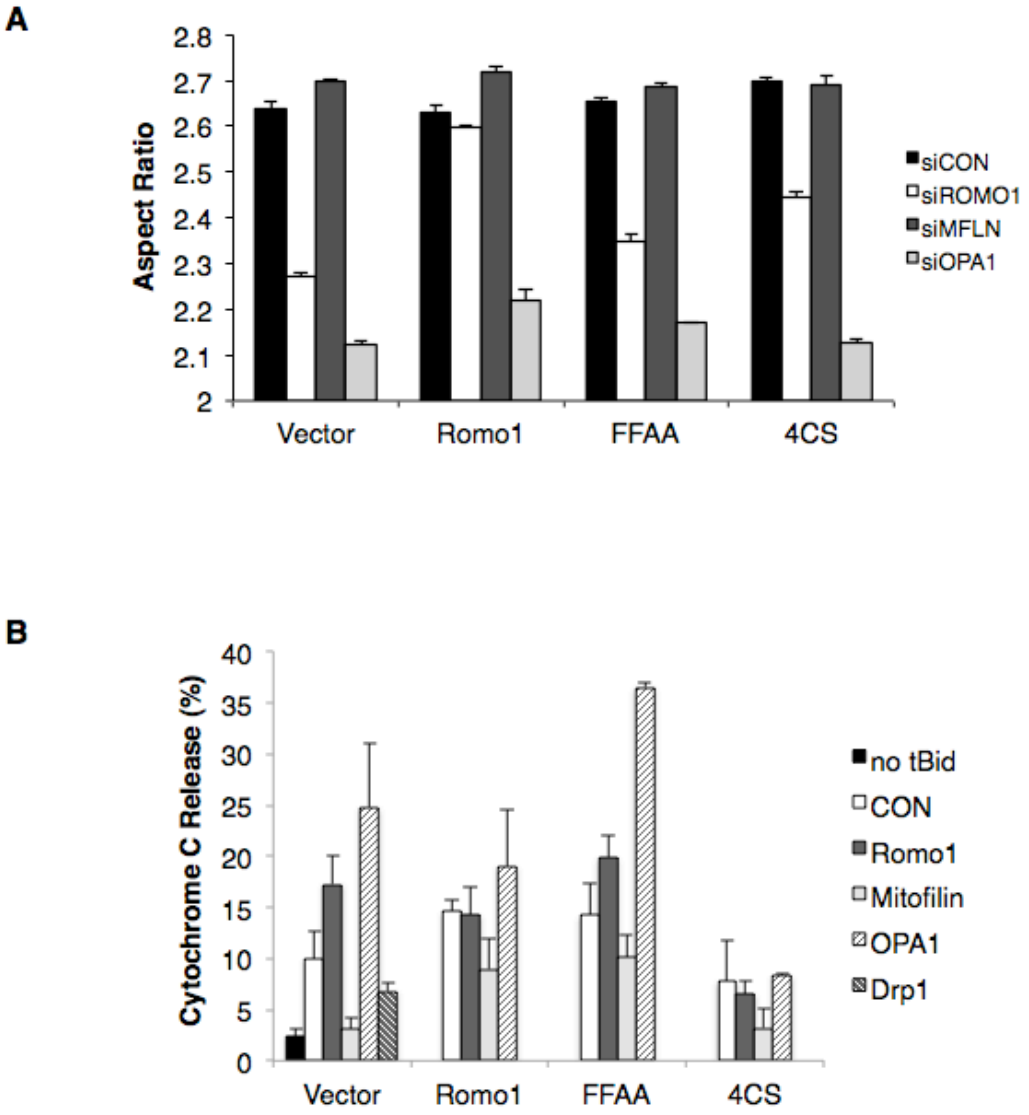

Figure 12 Romo1 REDOX status couples cristae junction maintenance to mitochondrial fusion A. Histogram showing the length:width (Aspect) ratio of the mitochondrial network in U20S cells transfected with either siCON, siRomo1, siMitofilin (siMFLN), or siOPA1 and infected 4h later with lentivirus encoding either empty vector, FLAG Romo1 WT, FFAA or 4CS. B. Histogram showing effect of knockdown of CON, Romo1, Mitofilin, OPA1 or Drp1 in U20S cells expressing either emtpy vector, FLAG-Romo1 WT, FFAA or 4CS on cytochrome C release 8hr after infection with Adeno-tBid.

suggesting that Mitofilin and OPA1 are downstream of Romo1 with respect to mitochondrial fusion. In Figure 12B, we used sensitivity to tBid-induced cytochrome C release as a proxy to evaluate the integrity of cristae junctions. We observed several unpredicted results. Firstly, knockdown of Mitofilin blocked tBid-induced cytochrome C release more strongly than knockdown of Drp1. As previously published, knockdown of OPA1 enhanced cytochrome C release (100). Surprisingly, Romo1-4CS expression was able to block cytochrome C release in the absence of OPA1 and expression of Romo1-FFAA enhanced cytochrome C release in the absence of OPA1, greater than OPA1 knockdown alone. These data place Romo1 downstream of OPA1 with respect to cristae junction integrity and lead to a model, whereby Romo1 mediates a REDOX-sensitive cristae junction checkpoint prior to mitochondrial fusion, summarized in Figure 13 and discussed below.

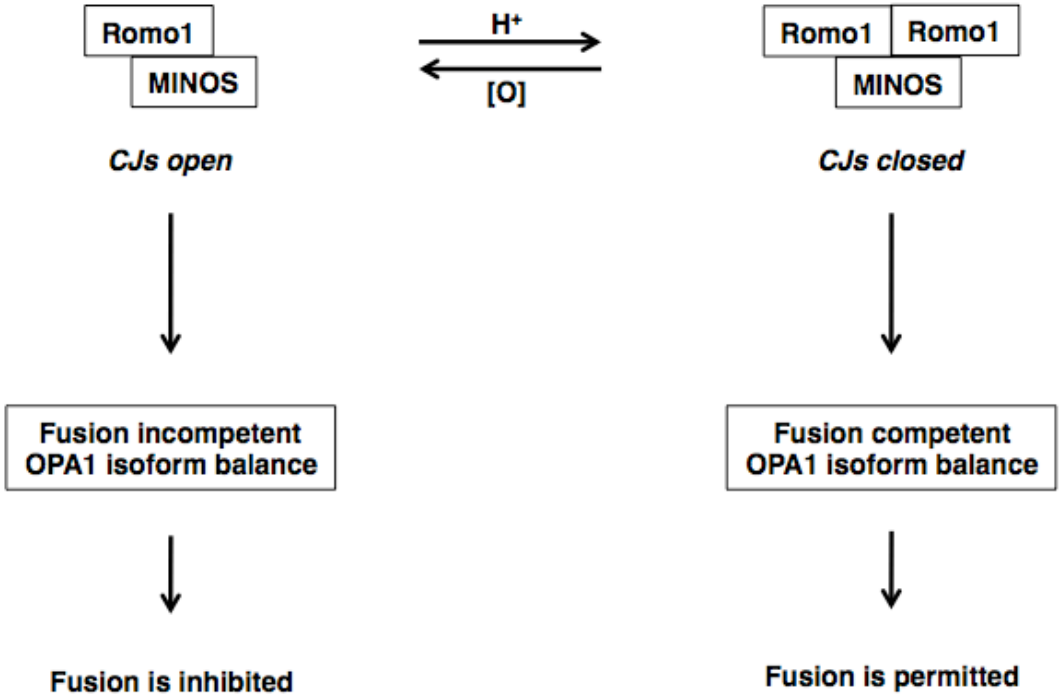

Figure 13 Romo1 mediates a cristae junction checkpoint prior to inner membrane fusion. A model depicting the findings described in this study. Based on our findings, we propose that Romo1 REDOX status regulates cristae junction closure, required for an OPA1 isoform balance permissive of mitochondrial fusion.

Chapter 4 Discussion

4.1 Romo1 is a novel regulator of mitochondrial fusion

Here we report the first genome-wide RNAi screen in mammalian cells looking for novel regulators of mitochondrial morphology. We used an unbiased, standardized algorithm adapted from a morphological bioapplication provided with the Cellomics vHCS Scan image analysis software to quantify the status of the mitochondrial network within each condition of the screen. This method proved more reliable than qualitative image analysis subject to human error and bias, issues that are being explored by others in this field (218). Using this approach we identified Romo1 as an essential mediator of mitochondrial fusion and cristae integrity. When using RNA interference as a screening tool, one must be wary of the likelihood of off-target effects. We employed a number of control strategies (*Reviewed in (219)*) to properly validate Romo1 as a hit. Knockdown of Romo1 yielded mitochondrial fragmentation with three different siRNA duplexes relative to a nontargeting siCONTROL. The duplex with the most robust phenotype was functionally validated at the mRNA level (Appendix IIIB) and in the absence of an endogenous antibody was also validated at the level of an exogenous FLAG-tagged Romo1 in Figure 8D. Importantly, exogenous FLAG-Romo1 was engineered to be resistant to the siRNA duplex through mutation of the seed sequence at wobble nucleotides, and this construct was able to functionally rescue normal mitochondrial morphology in the presence of Romo1 siRNA. Mutation of critical residues in the C-terminus of Romo1 abolished the

ability of this rescue construct to restore normal mitochondrial morphology at equal levels of expression. Validation of this candidate, using these criteria, identified Romo1 as a bona fide regulator of mitochondrial morphology. Mechanistically, we show that Romo1 regulates mitochondrial shape in concert with the inner membrane fusion GTPase, Opa1 and the recently described MINOS complex required for structural maintenance of cristae junctions. We propose that Romo1 couples REDOX signaling to mitochondrial morphology through a CJ checkpoint, required for normal OPA1 isoform balance and activity, and provide the mechanistic support for this below.

4.2 Romo1 couples mitochondrial REDOX to mitochondrial morphology

Loss of Romo1 results in two major morphological defects at the level of mitochondria: fragmentation of the mitochondrial network and loss of cristae. As expected, these morphological changes result in other mitochondrial defects including decreased respiratory fitness and sensitization to cytochrome C release and downstream apoptosis in the presence of apoptotic stimuli. We hypothesize that ROMO1 acts in concert with Mitofilin and the MINOS complex to maintain mitochondrial cristae integrity and hold CJs close. Mitofilin co-immunoprecipitates with FLAG-Romo1 indicating these proteins form a complex. Cells lacking Romo1 contain mitochondria either devoid of cristae or containing cristae stacks, the latter of which phenocopies Mitofilin mutant yeast strains (107). We hypothesize that ROMO1 acts in concert with OPA1 to mediate IMM fusion. Knockdown of both Romo1 and OPA1 cause dramatic mitochondrial

fragmentation. OPA1 requires a balance between long and processed isoforms to mediate fusion and cells lacking Romo1 have an imbalance of OPA1 isoforms. Finally, overexpression of OPA1 in cells lacking Romo1 partially restores normal mitochondrial morphology. The role of Romo1 in regulating mitochondrial shape appears to be regulated at the levels of mitochondrial REDOX. Under steady state conditions, FLAG-Romo1 exists in a ~10kDa, reduced state, as well as a highly oxidize state apparent by the presence of Romo1 species laddering up to > 245 kDa on non-reducing gels. Interestingly, the nonfunctional Romo1 mutant (Romo1-FFAA) is more highly oxidized that wild-type Romo1. Mutation of all four cysteine residues to the REDOX-insensitive residue serine, renders FLAG-Romo1-4CS completely reduced. While overexpression of FLAG-Romo1-WT does not alter mitochondrial morphology, overexpression of FLAG-Romo1-FFAA causes mild fragmentation and overexpression of FLAG-Romo1-4CS leads to elongation of the mitochondrial network indicating Romo1 is functionally and constitutively active in its reduced state and conversely inactive, with respect to mitochondrial fusion, in its oxidized state. Mitochondrial REDOX alters the balance between oxidized and reduced Romo1, as knockdown of glutathione reductase (GSR) with an shRNA increases Romo1 oxidation (Appendix IV), supporting this mechanism of Romo1 regulation within the cell. These results suggest that Romo1 actively couples mitochondrial REDOX to the regulation of mitochondrial morphology in a model proposed below.

4.3 Romo1 as a CJ-checkpoint protein required for mitochondrial fusion

When reduction of Romo1 is favored, Romo1 more strongly associates with Mitofilin, promoting mitochondrial fusion in a manner dependent on Opa1. When oxidization of Romo1 is favored, such as the Romo1-FFAA mutant, Romo1 is functionally inactive, leading to Opa1 isoform imbalance and impaired mitochondrial fusion. These results support a model whereby OPA1 is downstream of Romo1 with respect to mitochondrial fusion. Interestingly, evaluating cristae junction integrity, through a cytochrome C release assay, shows that FLAG-Romo1-4CS can inhibit cytochrome C release in the absence of OPA1, suggesting Romo1 is downstream of OPA1 with respect to cristae junction closure and that CJ closure and mitochondrial fusion are coupled. These results support a model whereby, in the absence of Romo1, cristae junctions are poorly maintained and mitochondria lose cristae, as in Figure 4A. In the absence of cristae, mitochondria are sensitized to apoptosis due to the inability to sequester proapoptotic molecules such as cytochrome C. We propose that in this sensitive state, OPA1 is inactivated to inhibit outer membrane reorganization, which could allow for cytochrome C release and accidental initiation of cell death pathways, during lipid remodeling. In this model, Romo1 is required to ensure cristae junctions are closed and cytochrome C sequestered, prior to mitochondrial fusion. This would serve as a checkpoint ensuring that mitochondrial fusion does not proceed if cristae junctions are open.

Surprisingly, knockdown of Mitofilin leads to mitochondrial elongation. Furthermore, knockdown of Romo1 and Mitofilin result in different imbalances of Opa1 isoforms. While knockdown of Romo1, Mitofilin and OPA1 all lead to cristae defects (Figure 4 and (100, 107)), the results are phenotypically different. Mitochondria lacking Romo1 are mostly devoid of cristae, with a small subset displaying cristae stacks identified in Figure 4A (arrow), which are characterized by sub-mitochondrial compartments that are completely closed, lacking cristae junctions, and are discontiguous with the inner membrane and intermembrane space. Mitochondria lacking Mitofilin, and other MINOS members, display cristae stacks (107), while loss of OPA1 leads to widening of cristae junctions (100). These observations are consistent with our findings. Knockdown of OPA1 leads to enhanced cytochrome C release and mitochondrial fragmentation. Knockdown of Mitofilin, however, blocks tBid-induced cytochrome C release. This is likely because the cristae stacks in mitochondria lacking Mitofilin are closed, and discontiguous with the intermembrane space, sequestering cytochrome C in a fashion that can no longer be dynamically regulated by apoptotic stimuli. As previously mentioned, loss of Mitofilin also causes mitochondrial elongation. This is consistent with a cristae junction checkpoint model. Loss of Mitofilin sequesters cytochrome C in closed cristae stacks devoid of cristae junctions. These mitochondria would be in a state constitutively permissive to mitochondrial fusion since there is no risk of cytochrome C release during outer membrane remodeling. Consistent with this hypothesis, OPA1 isoform balance is altered in a

manner conducive to mitochondrial fusion. Based on these observations, we propose the model summarized in Figure 13, whereby Romo1 couples mitochondrial REDOX to a cristae junctions closure checkpoint required for mitochondrial fusion, through MINOS and OPA1.

4.4 Future Directions

The model presented above raises many questions about the role of Romo1 in mitochondrial dynamics. Future work might explore some of the ideas, described below, among others. Firstly, the idea that Romo1 is regulated by mitochondrial REDOX raises a couple of questions. Is mitochondrial fusion directly linked to REDOX status or are there specific stimuli regulating Romo1-mediated mitochondrial fusion? Testing a panel of ROS inducers and correlating Romo1 REDOX status with mitochondrial shape will help to answer this question. Also, orienting Romo1 within the inner membrane will help to understand whether it is REDOX within the matrix or the intermembrane space that is regulating the two exposed cysteine residues likely to govern the REDOX sensitivity of Romo1. Secondly, is MINOS dynamically regulated? Thus far, no post-translational modifications or regulatory mechanisms of MINOS functions have been described. This is the first report of a dynamic interaction between MINOS and another protein. To date, reports have merely suggested MINOS is a structural requirement for cristae formation and maintenance and reports have focused on the requirement of MINOS for mitochondrial import and assembly of outer membrane complexes (220, 221); however, given the dynamics nature of cristae

junctions, it is likely that MINOS is regulated by mitochondrial health and function. To fully understand the roles of MINOS and Romo1 in mitochondrial fusion, it will be critical to understand how they regulate OPA1. Here, we report that knockdown of Romo1 and MINOS both cause OPA1 isoform imbalance. It will be important to reveal whether this result is a direct effect regulation of the proteases responsible for OPA1 processing, or if the isoform imbalance observed is due to the defects in cristae morphology, causing the spatial distribution of OPA1 to be altered resulting in differential processing. Given how little is known about Romo1, there are many questions that could be posed about its function. Assessing the physiological requirements of Romo1 by studying a Romo1 conditional knockout mouse model will help to direct future work to the most relevant roles of Romo1 within the mitochondria.

Given that the reports on MINOS function are largely centered on mitochondrial import, the role of Romo1 in this context will need to be addressed. MINOS has also been proposed to act as a large scaffold regulating numerous mitochondrial functions as it has been shown to associate not only with import proteins but also with the Voltage-dependent anion channel (VDAC1), the fusion component Ugo1, and with ERMES, a complex responsible for ER-mitochondrial communication through calcium and phospholipid exchange (222). *Van der Laan et al. (2012)* have proposed that a larger complex exists between MINOS and ERMES, termed ER-mitochondria organizing network (ERMIONE) (222), which may regulate numerous mitochondrial processes. While little evidence for this

complex has been reported, it could be important to future work with Romo1, given the emerging importance of the ER in regulating mitochondrial morphology.

4.5 Romo1 and cell death

While this report primarily describes the role of Romo1 in mitochondrial morphology, we also report several lines of evidence that Romo1 actively regulates apoptosis at the level of cristae junctions and cytochrome C release. We have shown that cells lacking Romo1 are sensitized to apoptotic stimuli-induced cytochrome C release, correlating with cell death as measured by condensed apoptotic nuclear morphology (Figure 5A-D). Interestingly, Romo1 is upregulated in a subset of cancer cells and can contribute to transformation (www.cbioportal.org and (204, 211)). Romo1 could serve as a potential therapeutic target if its upregulation leads to an inhibition of cytochrome C release in the presence of apoptotic signals. The observation that Romo1 regulates mitochondrial morphology in a manner coupled to cytochrome C release and apoptosis is of additional interest in the field of mitochondrial dynamics. A general consensus in the field is that mitochondrial fragmentation is either required for, or occurs simultaneous to, cytochrome C release (*Reviewed in (4, 223-225)*). We evaluated this concept by screening our list of candidate genes from the screen for sensitivity to tBid-induced cytochrome C release. Appendix VIIA shows that of 18 candidates that when knocked down give a fragmentation phenotype, knockdown of only 3 (Romo1, DNAJA3 and UNC5A) sensitize cells to tBid-induced cytochrome C release. Conversely, knockdown of

only 2 out of the 7 (RABGAP1 and AKR1B1) candidates with an elongation phenotype, also protected cells from tBid-induced cytochrome C release. Furthermore, Appendix VIIB shows that sensitivity to tBid-induced cytochrome C release does not correlate with downstream cell death as measured by condensed nuclei, suggesting that there is a low threshold of cytochrome C release required to initiate apoptosis. Interestingly, Romo1 was one of the few genes that acted as the literature would have predicted. Cells lacking Romo1 have fragmented mitochondria, are sensitized to cytochrome C release and downstream apoptosis. In this report, we primarily use sensitivity to cytochrome C release as a readout for CJ integrity and use condensed nuclei as a bona fide readout of cell death. Taken together, these data suggest that the mechanisms regulating mitochondrial morphology and apoptosis may be more intricate than previously thought.

4.6 Concluding Remarks

Using an unbiased genome-wide RNAi screening approach, we identified Romo1 as a regulator of mitochondrial fusion and cristae integrity. Romo1 is a REDOX-regulated mitochondrial inner membrane protein involved in interactions between the structural cristae junction complex MINOS, and the dynamically regulated fusion GTPase OPA1. Through these interactions, we propose that Romo1 couples mitochondrial REDOX signaling to a cristae junction checkpoint, ensuring that CJs are closed prior to outer membrane remodeling during fusion. Future work will assess the roles of Romo1 in a physiological context.

Chapter 5 References

1. Battelli, F., and Stern, L. (1912) Ergeb. Physiol. 15, 96-268.
2. Warburg, O. (1913) Arch. Gesamte. Physiol. 154, 599-617.
3. Ernster, L., and Schatz, G. (1981) Mitochondria: a historical review. J Cell Biol 91(3), 227s-255s.
4. Martinou, J.C. and R.J. Youle (2011) Mitochondria in apoptosis: Bcl-2 family members and mitochondrial dynamics. Dev Cell 21(1), 92-101.
5. Nunnari, J., and Suomalainen, A. (2012) Mitochondria: In Sickness and in Health. Cell 148, 1145-1159.
6. Grimm, S. (2012) The ER-mitochondria interface: The social network of cell death. Biochim Biophys Acta 1823, 327-334.
7. Turrens, J.F. (2003) Mitochondrial formation of reactive oxygen species. J Physiol 552(Pt 2), 335-344.
8. de Keizer, P.L.J., Burgering, B.M., and Dansen, T.B. (2011) Forkhead Box O as a Sensor, Mediator, and Regulator of Redox Signaling. Antioxid Redox Signal 14(6), 1093-1106.
9. Skulachev, V.P. (1997) Membrane-linked systems preventing superoxide formation. Biosci Rep 17(3), 347-366.
10. Farber, J.L. (1994) Mechanisms of cell injury by activated oxygen species. Environ Health Perspect 102(Suppl 10), 17-24.
11. Adler, V., Yin, Z., Tew, K.D., and Ronai, Z. (1999) Role of redox potential and reactive oxygen species in stress signaling. Oncogene 18(45), 6104-6111.
12. Bae, Y.S., Oh, H., Rhee, S.G., and Yoo, Y.D. (2011) Regulation of Reactive Oxygen Species Generation in Cell Signaling. Mol Cells 32(6), 491-509.
13. Bivona, T.G., Quatela, S.E., Bodermann, B.O., Ahearn, I.M., Soskis, M.J., Mor, A., Miura, J., Wiener, H.H., Wright, L., Saba, S.G., et al. (2006) PKC regulates a farnesyl-electrostatic switch on K-Ras that promotes its association with Bcl-XL on mitochondria and induces apoptosis. Mol Cell 21(4), 481-493.
14. Mihara, M., Erster, S., Zaika, A., Petrenko, O., Chittenden, T., Pancoska, P., and Moll, U.M. (2003) p53 has a direct apoptogenic role at the mitochondria. Mol Cell 11(3), 577-90.
15. Seth, R.B., Sun, L., Ea, C.K., and Chen, Z.J. (2005) Identification and characterization of MAVS, a mitochondrial antiviral signaling protein that activates NF-kappaB and IRF3. Cell 122, 669-682.
16. Meylan, E., Curran, J., Hofmann, K., Moradpour, D., Binder, M., Bartenschlager, R., and Tschopp, J. (2005) Cardif is an adaptor protein in the RIG-I antiviral pathway and is targeted by hepatitis C virus. Nat Immunol 437, 1167-1172.
17. Kawai, T., Takahashi, K., Sato, S., Coban, C., Kumar, H., Kato, H., Ishii, K.J., Takeuchi, O., and Akira, S. (2005) IPS-1, an adaptor triggering RIG-I- and Mda5-mediated type I interferon induction. Nat Immunol 6, 981-988.
18. Xu, L.G., Wang, Y.Y., Han, K.J., Li, L.Y., Zhai, Z., and Shu, H.B. (2005) VISA is an adapter protein required for virus-triggered IFN-beta signaling. Mol Cell 19, 727-740.

19. Kornmann, B., and Walter, P. (2010) ERMES-mediated ER-mitochondria contacts: molecular hubs for the regulation of mitochondrial biology. J Cell Sci 123(9), 1389-1393.
20. Friedman, J.R., Lackner, L.L., West, M., DiBenedetto, J.R., Nunnari, J., and Voeltz, G.K. (2011) ER tubules mark sites of mitochondrial division. Science 334(6054), 358-362.
21. McBride, H.M., et al. (2006) Mitochondria: more than just a powerhouse. Curr Biol 16(14), R551-560.
22. Argyropoulos, G., and Harper, M.E. (2002) Uncoupling proteins and thermoregulation. J Appl Physiol 92(5), 2187-2198.
23. Bereiter-Hahn, J., and Voth, M. (1994) Dynamics of Mitochondria in Living Cells: Shape Changes, Dislocations, Fusion and Fission of Mitochondria. Microsc Res Tech 27, 198-219.
24. Hales, K.G., and Fuller, M.T. (1997) Developmentally regulated mitochondrial fusion mediated by a conserved, novel, predicted GTPase. Cell 90(1), 121-129.
25. Hermann, G.J., Thatcher, J.W., Mills, J.P., Hales, K.G., Fuller, M.T., Nunnari, J., Shaw, J.M. (1998) Mitochondrial fusion in yeast requires the transmembrane GTPase Fzo1p. J Cell Biol 143(2), 359-373.
26. Santel, A., and Fuller, M.T. (2001) Control of mitochondrial morphology by a human mitofusin. J Cell Sci 114(Pt 5), 867-874.
27. Meeusen, S., DeVay, R., Block, J., Cassidy-Stone, A., Wayson, S., McCaffery, J.M., and Nunnari, J. (2006) Mitochondrial inner-membrane fusion and crista maintenance requires the dynamin-related GTPase Mgm1. Cell 127(2), 383-395.
28. Koshiba, T., Detmer, S.A., Kaiser, J.T., Chen, H., McCaffery, J.M., and Chan, D.C. (2004) Structural Basis of Mitochondrial Tethering by Mitofusin Complexes. Science 305(5685), 858-862.
29. Choi, S.Y., et al. (2006) A common lipid links Mfn-mediated mitochondrial fusion and SNARE-regulated exocytosis. Nat Cell Biol 8(11), 1255-62.
30. Jensen, R.E. and H. Sesaki (2006) Ahead of the curve: mitochondrial fusion and phospholipase D. Nat Cell Biol 8(11), 1215-7.
31. Detmer, S.A., and Chan, D.C. (2007) Complementation between mouse Mfn1 and Mfn2 protects mitochondrial fusion defects caused by CMT2A disease mutations. J Cell Biol 176(4), 405-414.
32. Ishihara, N., Eura, Y., and Mihara, K. (2004) Mitofusin 1 and 2 play distinct roles in mitochondrial fusion reactions via GTPase activity. J Cell Sci 117(Pt 26), 6535-6546.
33. Chen, H., Detmer, S.A., Ewald, A.J., Griffin, E.E., Fraser, S.E. and Chan, D.C. (2003) Mitofusins Mfn1 and Mfn2 coordinately regulate mitochondrial fusion and are essential for embryonic development. J Cell Biol 160(2), 189-200.
34. Hoppins, S., Edlich, F., Cleland, M.M., Banerjee, S., McCaffery, J.M., Youle, R.J., and Nunnari, J. (2011) The soluble form of Bax regulates mitochondrial fusion via MFN2 homotypic complexes. Mol Cell 41(2), 150-160.

35. Eura, Y., et al. (2006) Identification of a novel protein that regulates mitochondrial fusion by modulating mitofusin (Mfn) protein function. J Cell Sci 119(Pt 23), 4913-25.
36. Cipolat, S., Martins de Brito, O., Dal Zilla, B., and Scorrano, L. (2004) OPA1 requires mitofusin 1 to promote mitochondrial fusion. Proc Natl Acad Sci U S A 101(45), 15927-15932.
37. Delettre, C., Griffoin, J.M., Kaplan, J., Dollfus, H., Lorenz, B., Faivre, L, Lenaers, G., Belenguer, P., and Hamel, C.P. (2001) Mutation spectrum and splicing variants in the OPA1 gene. Hum Genet 109(6), 584-591.
38. Ishihara, N., Fujita, Y., Oka, T., and Mihara, K. (2006) Regulation of mitochondrial morphology through proteolytic cleave of Opa1. EMBO J 25(13), 2966-2977.
39. Waterston, R.H., et al. (2002) Initial sequencing and comparative analysis of the mouse genome. Nature 420(6915), 520-62.
40. Song, Z., et al. (2007) OPA1 processing controls mitochondrial fusion and is regulated by mRNA splicing, membrane potential, and Yme1L. J Cell Biol 178(5), 749-755.
41. DeVay, R.M., Dominguez-Ramirez, L., Lackner, LL., Hoppins, S., Stahlberg, H., and Nunnari, J. (2009) Coassembly of Mgm1 isoforms requires cardiolipin and mediates mitochondrial inner membrane fusion. J Cell Biol 186(6), 793-803.
42. Griparic, L., Kanazawa, T., and van der Bliek, A.M. (2007) Regulation of the mitochondrial dynamin-like protein Opa1 by proteolytic cleavage. J Cell Biol 178(5), 757-764.
43. Cipolat, S., Rudka, T., Harmann, D., Costa, V., Serneels, L., Craessaerts, K., Metzger, K., Frezza, C., Annaert, W., D'Adamio, L., et al. (2006) Mitochondrial rhomboid PARL regulates cytochrome c release during apoptosis via OPA1-dependent cristae remodeling. Cell 126(1), 163-175.
44. Duvezin-Caubet, S., Koppen, M., Wagener, J., Zick, M., Israel, L., Bernacchia, A., Jagasia, R., Rugarli, E.I., Imhof, A., Neupert, W., et al. (2007) OPA1 processing reconstituted in yeast depends on the subunit composition of the m-AAA protease in mitochondria. Mol Biol Cell 18(9), 3582-3590.
45. Ehses, S., Raschke, I., Mancuso, G., Bernacchia, A., Geimer, S., Tondera, D., Martinou, J.C., Westermann, B., Rugarli, E.I, and Langer, T. (2009) Regulation of OPA1 processing and mitochondrial fusion by m-AAA protease isoenzymes and OMA1. J Cell Biol 187(7), 1023-1036.
46. Head, B., et al. (2009) Inducible proteolytic inactivation of OPA1 mediated by the OMA1 protease in mammalian cells. J Cell Biol 187(7), 959-966.
47. Sesaki, H. and R.E. Jensen (2001) UGO1 encodes an outer membrane protein required for mitochondrial fusion. J Cell Biol 152(6), 1123-34.
48. Sesaki, H. and R.E. Jensen (2004) Ugo1p links the Fzo1p and Mgm1p GTPases for mitochondrial fusion. J Biol Chem 279(27), 28298-303.
49. Hoppins, S., et al. (2009) Mitochondrial outer and inner membrane fusion requires a modified carrier protein. J Cell Biol 184(4), 569-81.

50. Smirnova, E., Shurland, D.L., Ryazantsev, S.N., and van der Bliek, A.M. (1998) A human dynamin-related protein controls the distribution of mitochondria. J Cell Biol 143(2), 351-358.
51. Bleazard, W., McCaffery, J.M., King, E.J., Bale, S., Mozdy, A., Tieu, Q., Nunnari, J., Shaw, J.M. (1999) The dynamin-related GTPase Dnm1 regulates mitochondrial fission in yeast. Nat Cell Biol 1(5), 298-304.
52. Smirnova, E., Griparic, L., Shurland, D.L., and van der Bliek, A.M. (2001) Dynamin-related protein Drp1 is required for mitochondrial division in mammalian cells. Mol Biol Cell 12(8), 2245-2256.
53. Ingerman, E., Perkins, E.M., Marino, M., Mears, J.A., McCaffery, J.M., Hinshaw, J.E., and Nunnari, J. (2005) Dnm1 forms spirals that are structurally tailored to fit mitochondria. J Cell Biol 170(7), 1021-1027.
54. Mears, J.A., Lackner, L.L., Fang, S., Ingerman, E., Nunnari, J., and Hinshaw, J.E. (2011) Conformational changes in Dnm1 support a contractile mechanism for mitochondrial fission. Nat Struct Mol Biol 18(1), 20=26.
55. Tieu, Q., and Nunnari, J. (2000) Mdv1p Is a WD Repeat Protein that Interacts with the Dynamin-related GTPase, Dnm1p, to Trigger Mitochondrial Division. J Cell Biol 151(2), 353-366.
56. Tieu, Q., Okreglak, V., Naylor, K., and Nunnari, J. (2002) The WD repeat protein, Mdv1p, functions as a molecular adaptor by interacting with Dnm1p and Fis1p during mitochondrial fission. J Cell Biol 2002(158), 3.
57. Griffin, E.E., et al. (2005) The WD40 protein Caf4p is a component of the mitochondrial fission machinery and recruits Dnm1p to mitochondria. J Cell Biol 170(2), 237-248.
58. Cerveny, K.L., Struder, S.L., Jensen, R.E., and Sesaki, H. (2007) Yeast mitochondrial division and distribution require the cortical num1 protein. Dev Cell 12(3), 363-375.
59. Hammermeister, M., Schodel, K., and Westermann, B. (2010) Mdm36 is a mitochondrial fission-promoting protein in Saccharomyces cerevisiae. Mol Biol Cell 21(14), 2443-2452.
60. Stojanovski, D., Koutsopoulos, O.S., Okamoto, K., and Ryan, M.T. (2004) Levels of human Fis1 at the mitochondrial outer membrane regulate mitochondrial morphology. J Cell Sci 117(Pt 7), 1201-1210.
61. James, D.I., Parone, P.A., Mattenberger, Y., and Martinou, J.C. (2003) hFis1, a novel component of the mammalian mitochondrial fission machinery. J Biol Chem 278(38), 36373-36379.
62. Yoon, Y., Krueger, E.W., Oswald, B.., and McNiven, M.A. (2003) The mitochondrial protein hFis1 regulates mitochondrial fission in mammalian cells through an interaction with the dynamin-like protein DLP1. Mol Cell Biol 23(15), 5409-5420.
63. Otera, H., Wang, C., Cleland, M.M., Setoguchi, K., Yokota, S., Youle, R.J., and Mihara, K. (2010) Mff is an essential factor for mitochondrial recruitment of Drp1 during mitochondrial fission in mammalian cells. J Cell Biol 191(6), 1141-1158.

64. Lee, Y.J., Jeong, S.Y., Karbowski, M., Smith, C.L., and Youle, R.J. (2004) Roles of the Mammalian Mitochondrial Fission and Fusion Mediators Fis1, Drp1, and Opa1 in Apoptosis. Mol Biol Cell 15(11), 5001-5011.
65. Wasiak, S., Zunino, R., and McBride, H.M. (2007) Bax/Bak promote sumoylation of DRP1 and its stable association with mitochondria during apoptotic cell death. J Cell Biol 177(3), 439-450.
66. Gandre-Babbe, S., and van der Bliek, A.M. (2008) The novel tail-anchored membrane protein Mff controls mitochondrial and peroxisomal fission in mammalian cells. Mol Biol Cell 19(6), 2402-2412.
67. Palmer, C.S., Osellame, L.D., Laine, D., Koutsopoulos, O.S., Frazier, A.E., and Ryan, M.T. (2011) MiD49 and MiD51, new components of the mitochondrial fission machinery. EMBO Rep 12(6), 565-573.
68. Zhao, J., Liu, T., Jin, S., Wang, X., Qu, M., Uhlen, P., Tomilin, N., Shupliakov, O., Lendahl, U., and Nister, M. (2011) Human MIEF1 recruits Drp1 to mitochondrial outer membranes and promotes mitochondrial fusion rather than fission. EMBO J 30(14), 2762-2778.
69. Tondera, D., Santel, A., Schwarzer, R., Dames, S., Giese, K., Klippel, A., and Kaufmann, J. (2004) Knockdown of MTP18, a novel phosphatidylinositol 3-kinase-dependent protein, affects mitochondrial morphology and induces apoptosis. J Biol Chem 279(30), 31544-31555.
70. Tondera, D., Czauderna, F., Paulick, K., Schwarzer, R. Kaufmann, J., and Santel, A. (2005) The mitochondrial protein MTP18 contributes to mitochondrial fission in mammals. J Cell Sci 118(Pt 14), 3049-3059.
71. Niemann, A., Ruegg, M., La Padula, V., Schenone, A., and Suter, U. (2005) Ganglioside-induced differentiation associated protein 1 is a regulator of the mitochondrial network: new implications for Charcot-Marie-Tooth disease. J Cell Biol 170(7), 1067-1078.
72. Pedrola, L., Espert, A., Wu, X., Claramunt, R., Shy, M.E., and Palau, F. (2005) GDAP1, the protein causing Charcot-Marie-Tooth disease type 4A, is expressed in neurons and is associated with mitochondria. Hum Mol Genet 14(8), 1087-1094.
73. Karbowski, M., Jeong, S.Y., and Youle, R.J. (2004) Endophilin B1 is required for the maintenance of mitochondrial morphology. J Cell Biol 166(7), 1027-1039.
74. Rostovtseva, T.K., Boukari, H., Antignani, A., Shiu, B., Banerjee, S., Neutzner, A., and Youle, R.J. (2009) Bax activates endophilin B1 oligomerization and lipid membrane vesiculation. J Biol Chem 284(49), 34390-34399.
75. Chang, C.R. and C. Blackstone (2007) Cyclic AMP-dependent protein kinase phosphorylation of Drp1 regulates its GTPase activity and mitochondrial morphology. J Biol Chem 282(30), 21583-7.
76. Cereghetti, G.M., et al. (2008) Dephosphorylation by calcineurin regulates translocation of Drp1 to mitochondria. Proc Natl Acad Sci U S A 105(41), 15803-8.
77. Gomes, L.C., G. Di Benedetto, and L. Scorrano (2011) During autophagy mitochondria elongate, are spared from degradation and sustain cell viability. Nat Cell Biol 13(5), 589-98.

78. Taguchi, N., Ishihara, N., Jofuku, A., Oka, T., and Mihara, K. (2007) Mitotic phosphorylation of dynamin-related GTPase Drp1 participates in mitochondrial fission. J Biol Chem 282(15), 11521-11529.
79. Qi, X., et al. (2011) Aberrant mitochondrial fission in neurons induced by protein kinase C{delta} under oxidative stress conditions in vivo. Mol Biol Cell 22(2), 256-65.
80. Karbowski, M., A. Neutzner, and R.J. Youle (2007) The mitochondrial E3 ubiquitin ligase MARCH5 is required for Drp1 dependent mitochondrial division. J Cell Biol 178(1), 71-84.
81. Park, Y.Y., et al. (2010) Loss of MARCH5 mitochondrial E3 ubiquitin ligase induces cellular senescence through dynamin-related protein 1 and mitofusin 1. J Cell Sci 123(Pt 4), 619-26.
82. Wang, H., et al. (2011) Parkin ubiquitinates Drp1 for proteasome-dependent degradation: implication of dysregulated mitochondrial dynamics in Parkinson disease. J Biol Chem 286(13), 11649-58.
83. Harder, Z., R. Zunino, and H. McBride (2004) Sumo1 conjugates mitochondrial substrates and participates in mitochondrial fission. Curr Biol 14(4), 340-5.
84. Figueroa-Romero, C., et al. (2009) SUMOylation of the mitochondrial fission protein Drp1 occurs at multiple nonconsensus sites within the B domain and is linked to its activity cycle. FASEB J 23(11), 3917-27.
85. Braschi, E., R. Zunino, and H.M. McBride (2009) MAPL is a new mitochondrial SUMO E3 ligase that regulates mitochondrial fission. EMBO Rep 10(7), 748-54.
86. Zunino, R., et al. (2009) Translocation of SenP5 from the nucleoli to the mitochondria modulates DRP1-dependent fission during mitosis. J Biol Chem 284(26), 17783-95.
87. Zunino, R., et al. (2007) The SUMO protease SENP5 is required to maintain mitochondrial morphology and function. J Cell Sci 120(Pt 7), 1178-88.
88. Rizzuto, R., Pinton, P., Carrington, W., Fay, F.S., Fogarty, K.E., Lifshitz, L.M., Tuft, R.A., and Pozzan, T. (1998) Close contacts with the endoplasmic reticulum as determinants of mitochondrial Ca2+ responses. Science 280(5370), 1763-1766.
89. de Brito, O.M., and Scorrano, L. (2008) Mitofusin 2 tethers endoplasmic reticulum to mitochondria. Nature 456(7222), 605-610.
90. van der Laan, M., Bohnert, M., Widermann, N., and Pfanner, N. (2012) Role of MINOS in mitochondrial membrane architecture and biogenesis. Trends Cell Biol 22(4), 185-192.
91. Gilkerson, R.W., Selker, J.M., and Capaldi, R.A. (2003) The cristal membrane of mitochondria is the principal site of oxidative phosphorylation. FEBS Letters 546(2-3), 355-358.
92. Zick, M., Rabl, R., and Reichert, A.S. (2009) Cristae formation-linking ultrastructure and function of mitochondria. Biochim Biophys Acta 1793(1), 5-19.

93. Paumard, P., Vaillier, J., Coulary, B., Schaeffer, J., Soubannier, V., Mueller, D.M., Brethes, D., di Rago, J.P., and Velours, J. (2002) The ATP synthase is involved in generating mitochondrial cristae morphology. EMBO J 21(3), 221-230.
94. Arnold, I., Pfeiffer, K., Neupert, W., Stuart, R.A., and Schagger, H. (1998) Yeast mitochondrial F1F0-ATP synthase exists as a dimer: identification of three dimer-specific subunits. EMBO J 17(24), 7170-7178.
95. Schagger, H., and Pfeiffer, K. (200) Supercomplexes in the respiratory chains of yeast and mammalian mitochondria. EMBO J 19(8), 1777-1783.
96. Krause, F., Reifschneider, N.H., Goto, S., and Dencher, N.A. (2005) Active oligomeric ATP synthases in mammalian mitochondria. Biochem Biophys Res Commun 329(2), 583-590.
97. Strauss, M., Hofhaus, G., Schroder, R.R., and Kuhlbrandt, W. (2008) Dimer ribbons of ATP synthase shape the inner mitochondrial membrane. EMBO J 27(7), 1154-1160.
98. Olichon, A., Baricault, L., Gas, N., Guilou, E., Valette, A., Belenguer, P., and Lenaers, G. (2003) Loss of OPA1 perturbates the mitochondrial inner membrane structure and integrity, leading to cytochrome c release and apoptosis. J Biol Chem 278(10), 7743-7746.
99. Arnoult, D., Grodet, A., Lee, Y.J., Estaquier, J., and Blackstone, C. (2005) Release of Opa1 during apoptosis participates in the rapid and complete release of cytochrome c and subsequent mitochondrial fragmentation. J Biol Chem 280(42), 35742-35750.
100. Frezza, C., Cipolat, S., de Brito, O.M., Micaroni, M., Beznoussenko, G.V., Rudka, T., Bartoli, D., Polishuck, R., Danial, N.N., De Strooper, B., and Scorrano, L. (2006) OPA1 controls apoptotic cristae remodeling independently from mitochondrial fusion. Cell 126(1), 177-189.
101. John, G.B., Shang, Y., Li, L., Renken, C., Mannella, C.A., Selker, J.M., Rangell, L., Bennett, M.J., and Zha, J. (2005) The mitochondrial inner membrane protein mitofilin controls cristae morphology. Mol Biol Cell 16(3), 1543-1554.
102. Rabl, R., Soubannier, V., Scholz, R., Vogel, F., Mendl, N., Vasiljev-Neumeyer, A., Korner, C., Jagasia, R., Keil, T., Baumeister, W., Cyrklaff, M., Neupert, W., and Reichert, A.S. (2009) Formation of cristae and crista junctions in mitochondria depends on antagonism between Fcj1 and Su e/g. J Cell Biol 185(6), 1047-1063.
103. Mun, J.Y., Lee, T.H., Kim, J.H., Yoo, B.H., Bahk, Y.Y., Koo, H.S., and Han, S.S. (2010) Caenorhabditis elegans mitofilin homologs control the morphology of mitochondrial cristae and influence reproduction and physiology. J Cell Physiol 224(3), 748-756.
104. Darshi, M., Mendiola, V.L., Mackey, M.R., Murphy, A.N., Koller, A., Perkins, G.A., Ellisman, M.H., and Taylor, S.S. (2011) ChChd3, an inner mitochondrial membrane protein, is essential for maintaining crista integrity and mitochondrial function. J Biol Chem 286(4), 2918-2932.
105. Head, B.P., Zulaika, M., Ryazantsev, S., and van der Bliek, A.M. (2011) A novel mitochondrial outer membrane protein, MOMA-1, that affects crista morphology in Caenorhabditis elegans. Mol Biol Cell 22(6), 831-841.

106. Hoppins, S., Collins, S.R., Cassidy-Stone, A., Hummel, E., Devay, R.M., Lackner, L.L., Westermann, B., Schuldiner, M., Weissman, J.S., and Nunnari, J. (2011) A mitochondrial-focused genetic interaction map reveals a scaffold-like complex required for inner membrane organization in mitochondria. J Cell Biol 195(2), 323-340.
107. von der Malsburg, K., Muller, J.M., Bohnert, M., Oeljeklaus, S., Kwiatkowska, P., Becker, T., Loniewska-Lwowska, A., Wiese, S., Rao, S., Milenkovic, D., et al. (2011) Dual role of mitofilin in mitochondrial membrane organization and protein biogenesis. Dev Cell 21(4), 694-707.
108. Harner, M., Korner, C., Walther, D., Mokranjac, D., Kaesmacher, J., Welsch, U., Griffith, J., Mann, M., Reggiori, F., Neupert, W. (2011) The mitochondrial contact site complex, a determinant of mitochondrial architecture. EMBO J 30(21), 4356-4370.
109. Alkhaja, A.K., Jans, D.C., Nikolov, M., Vukotic, M., Lytovchenko, O., Ludewig, F., Schliebs, W., Riedel, D., Urlaub, H., Jakobs, S., and Deckers, M. (2012) MINOS1 is a conserved component of mitofilin complexes and required for mitochondrial function and cristae organization. Mol Biol Cell 23(2), 247-257.
110. Chen, H., McCaffery, J.M., and Chan, D.C. (2007) Mitochondrial fusion protects against neurodegeneration in the cerebellum. Cell 130(3), 548-562.
111. Gilkerson, R.W., et al. (2008) Mitochondrial nucleoids maintain genetic autonomy but allow for functional complementation. J Cell Biol 181(7), 1117-28.
112. Albring, M., J. Griffith, and G. Attardi (1977) Association of a protein structure of probable membrane derivation with HeLa cell mitochondrial DNA near its origin of replication. Proc Natl Acad Sci U S A 74(4), 1348-52.
113. Legros, F., Malka, F., Frachon, P., Lombes, A., and Rojo, M. (2004) Organization and dynamics of human mitochondrial DNA. J Cell Sci 117(Pt 13), 2653-2662.
114. Rebelo, A.P., L.M. Dillon, and C.T. Moraes (2011) Mitochondrial DNA transcription regulation and nucleoid organization. J Inherit Metab Dis 34(4), 941-51.
115. Solieri, L. (2010) Mitochondrial inheritance in budding yeasts: towards an integrated understanding. Trends Microbiol 18(11), 521-30.
116. Wikstrom, J.D., G. Twig, and O.S. Shirihai (2009) What can mitochondrial heterogeneity tell us about mitochondrial dynamics and autophagy? Int J Biochem Cell Biol 41(10), 1914-27.
117. Chen, H., A. Chomyn, and D.C. Chan (2005) Disruption of fusion results in mitochondrial heterogeneity and dysfunction. J Biol Chem 280(28), 26185-92.
118. Mizushima, N. and M. Komatsu (2011) Autophagy: renovation of cells and tissues. Cell 147(4), 728-41.
119. Kujoth, G.C., et al. (2005) Mitochondrial DNA mutations, oxidative stress, and apoptosis in mammalian aging. Science 309(5733), 481-4.
120. Trifunovic, A., et al. (2004) Premature ageing in mice expressing defective mitochondrial DNA polymerase. Nature 429(6990), 417-23.

121. Orr, W.C. and R.S. Sohal (1994) Extension of life-span by overexpression of superoxide dismutase and catalase in Drosophila melanogaster. Science 263(5150), 1128-30.
122. DiMauro, S., et al. (2002) Mitochondrial abnormalities in muscle and other aging cells: classification, causes, and effects. Muscle Nerve 26(5), 597-607.
123. Twig, G., et al. (2008) Fission and selective fusion govern mitochondrial segregation and elimination by autophagy. EMBO J 27(2), 433-46.
124. Narendra, D.P., et al. (2010) PINK1 is selectively stabilized on impaired mitochondria to activate Parkin. PLoS Biol 8(1), e1000298.
125. Greene, A.W., et al. (2012) Mitochondrial processing peptidase regulates PINK1 processing, import and Parkin recruitment. EMBO Rep 13(4), 378-85.
126. Kawajiri, S., et al. (2010) PINK1 is recruited to mitochondria with parkin and associates with LC3 in mitophagy. FEBS Lett 584(6), 1073-9.
127. Matsuda, N., et al. (2010) PINK1 stabilized by mitochondrial depolarization recruits Parkin to damaged mitochondria and activates latent Parkin for mitophagy. J Cell Biol 189(2), 211-21.
128. Vives-Bauza, C., et al. (2010) PINK1-dependent recruitment of Parkin to mitochondria in mitophagy. Proc Natl Acad Sci U S A 107(1), 378-83.
129. Clark, I.E., et al. (2006) Drosophila pink1 is required for mitochondrial function and interacts genetically with parkin. Nature 441(7097), 1162-6.
130. Park, J., et al. (2006) Mitochondrial dysfunction in Drosophila PINK1 mutants is complemented by parkin. Nature 441(7097), 1157-61.
131. Narendra, D., et al. (2010) p62/SQSTM1 is required for Parkin-induced mitochondrial clustering but not mitophagy; VDAC1 is dispensable for both. Autophagy 6(8), 1090-106.
132. Okatsu, K., et al. (2010) p62/SQSTM1 cooperates with Parkin for perinuclear clustering of depolarized mitochondria. Genes Cells 15(8), 887-900.
133. Pankiv, S., et al. (2007) p62/SQSTM1 binds directly to Atg8/LC3 to facilitate degradation of ubiquitinated protein aggregates by autophagy. J Biol Chem 282(33), 24131-45.
134. Tanaka, A., et al. (2010) Proteasome and p97 mediate mitophagy and degradation of mitofusins induced by Parkin. J Cell Biol 191(7), 1367-80.
135. Elmore, S. (2007) Apoptosis: a review of programmed cell death. Toxicol Pathol 35(4), 495-516.
136. Fulda, S. and K.M. Debatin (2006) Extrinsic versus intrinsic apoptosis pathways in anticancer chemotherapy. Oncogene 25(34), 4798-811.
137. Martinou, J.-C., and Youle, R.J. (2011) Mitochondria in Apoptosis: Bcl-2 Family Members and Mitochondrial Dynamics. Dev Cell 21, 92-101.
138. De Vos, K., et al. (1998) The 55-kDa tumor necrosis factor receptor induces clustering of mitochondria through its membrane-proximal region. J Biol Chem 273(16), 9673-80.
139. Mancini, M., et al. (1997) Mitochondrial proliferation and paradoxical membrane depolarization during terminal differentiation and apoptosis in a human colon carcinoma cell line. J Cell Biol 138(2), 449-69.
140. Frank, S., et al. (2001) The role of dynamin-related protein 1, a mediator of mitochondrial fission, in apoptosis. Dev Cell 1(4), 515-25.

141. Karbowski, M., et al. (2002) Spatial and temporal association of Bax with mitochondrial fission sites, Drp1, and Mfn2 during apoptosis. J Cell Biol 159(6), 931-8.
142. Lee, Y.J., et al. (2004) Roles of the mammalian mitochondrial fission and fusion mediators Fis1, Drp1, and Opa1 in apoptosis. Mol Biol Cell 15(11), 5001-11.
143. Sheridan, C., et al. (2008) Bax- or Bak-induced mitochondrial fission can be uncoupled from cytochrome C release. Mol Cell 31(4), 570-85.
144. Breckenridge, D.G., et al. (2008) Caenorhabditis elegans drp-1 and fis-2 regulate distinct cell-death execution pathways downstream of ced-3 and independent of ced-9. Mol Cell 31(4), 586-97.
145. Sugioka, R., S. Shimizu, and Y. Tsujimoto (2004) Fzo1, a protein involved in mitochondrial fusion, inhibits apoptosis. J Biol Chem 279(50), 52726-34.
146. Karbowski, M., et al. (2004) Quantitation of mitochondrial dynamics by photolabeling of individual organelles shows that mitochondrial fusion is blocked during the Bax activation phase of apoptosis. J Cell Biol 164(4), 493-9.
147. Tondera, D., et al. (2009) SLP-2 is required for stress-induced mitochondrial hyperfusion. EMBO J 28(11), 1589-600.
148. Baricault, L., et al. (2007) OPA1 cleavage depends on decreased mitochondrial ATP level and bivalent metals. Exp Cell Res 313(17), 3800-8.
149. Merkwirth, C., et al. (2008) Prohibitins control cell proliferation and apoptosis by regulating OPA1-dependent cristae morphogenesis in mitochondria. Genes Dev 22(4), 476-88.
150. Ly, C.V. and P. Verstreken (2006) Mitochondria at the synapse. Neuroscientist 12(4), 291-9.
151. Frederick, R.L., K. Okamoto, and J.M. Shaw (2008) Multiple pathways influence mitochondrial inheritance in budding yeast. Genetics 178(2), 825-37.
152. Frederick, R.L. and J.M. Shaw (2007) Moving mitochondria: establishing distribution of an essential organelle. Traffic 8(12), 1668-75.
153. Saxton, W.M. and P.J. Hollenbeck (2012) The axonal transport of mitochondria. J Cell Sci 125(Pt 9), 2095-104.
154. Fransson, A., A. Ruusala, and P. Aspenstrom (2003) Atypical Rho GTPases have roles in mitochondrial homeostasis and apoptosis. J Biol Chem 278(8), 6495-502.
155. Fransson, S., A. Ruusala, and P. Aspenstrom (2006) The atypical Rho GTPases Miro-1 and Miro-2 have essential roles in mitochondrial trafficking. Biochem Biophys Res Commun 344(2), 500-10.
156. Liu, X. and G. Hajnoczky (2009) Ca2+-dependent regulation of mitochondrial dynamics by the Miro-Milton complex. Int J Biochem Cell Biol 41(10), 1972-6.
157. Glater, E.E., et al. (2006) Axonal transport of mitochondria requires milton to recruit kinesin heavy chain and is light chain independent. J Cell Biol 173(4), 545-57.

158. Brickley, K., et al. (2005) GRIF-1 and OIP106, members of a novel gene family of coiled-coil domain proteins: association in vivo and in vitro with kinesin. J Biol Chem 280(15), 14723-32.
159. Smith, M.J., et al. (2006) Mapping the GRIF-1 binding domain of the kinesin, KIF5C, substantiates a role for GRIF-1 as an adaptor protein in the anterograde trafficking of cargoes. J Biol Chem 281(37), 27216-28.
160. Misko, A., et al. (2010) Mitofusin 2 is necessary for transport of axonal mitochondria and interacts with the Miro/Milton complex. J Neurosci 30(12), 4232-40.
161. Weihofen, A., et al. (2009) Pink1 forms a multiprotein complex with Miro and Milton, linking Pink1 function to mitochondrial trafficking. Biochemistry 48(9), 2045-52.
162. Saotome, M., et al. (2008) Bidirectional Ca2+-dependent control of mitochondrial dynamics by the Miro GTPase. Proc Natl Acad Sci U S A 105(52), 20728-33.
163. Kraus, B. and H. Cain (1980) Giant mitochondria in the human myocardium--morphogenesis and fate. Virchows Arch B Cell Pathol Incl Mol Pathol 33(1), 77-89.
164. Coleman, R., et al. (1987) Giant mitochondria in the myocardium of aging and endurance-trained mice. Gerontology 33(1), 34-9.
165. Kanzaki, Y., et al. (2010) Giant mitochondria in the myocardium of a patient with mitochondrial cardiomyopathy: transmission and 3-dimensional scanning electron microscopy. Circulation 121(6), 831-2.
166. Beraud, N., et al. (2009) Mitochondrial dynamics in heart cells: very low amplitude high frequency fluctuations in adult cardiomyocytes and flow motion in non beating Hl-1 cells. J Bioenerg Biomembr 41(2), 195-214.
167. Chen, L., et al. (2009) Mitochondrial OPA1, apoptosis, and heart failure. Cardiovasc Res 84(1), 91-9.
168. Ashrafian, H., et al. (2010) A mutation in the mitochondrial fission gene Dnm1l leads to cardiomyopathy. PLoS Genet 6(6), e1001000.
169. Ong, S.B., et al. (2010) Inhibiting mitochondrial fission protects the heart against ischemia/reperfusion injury. Circulation 121(18), 2012-22.
170. Hanahan, D. and R.A. Weinberg (2000) The hallmarks of cancer. Cell 100(1), 57-70.
171. Galluzzi, L., et al. (2010) Mitochondrial gateways to cancer. Mol Aspects Med 31(1), 1-20.
172. Warburg, O. (1956) On the origin of cancer cells. Science 123(3191), 309-314.
173. Fulda, S. and G. Kroemer (2011) Mitochondria as therapeutic targets for the treatment of malignant disease. Antioxid Redox Signal 15(12), 2937-49.
174. Tandler, B. and C.L. Hoppel (1986) Studies on giant mitochondria. Ann N Y Acad Sci 488, 65-81.
175. Terman, A. and U.T. Brunk (2005) The aging myocardium: roles of mitochondrial damage and lysosomal degradation. Heart Lung Circ 14(2), 107-14.

176. Murakoshi, M., Y. Osamura, and K. Watanabe (1985) Mitochondrial alterations in aged rat adrenal cortical cells. Tokai J Exp Clin Med 10(5), 531-6.
177. Lee, S., et al. (2007) Mitochondrial fission and fusion mediators, hFis1 and OPA1, modulate cellular senescence. J Biol Chem 282(31), 22977-83.
178. Mai, S., et al. (2010) Decreased expression of Drp1 and Fis1 mediates mitochondrial elongation in senescent cells and enhances resistance to oxidative stress through PINK1. J Cell Sci 123(Pt 6), 917-26.
179. Yoon, Y.S., et al. (2006) Formation of elongated giant mitochondria in DFO-induced cellular senescence: involvement of enhanced fusion process through modulation of Fis1. J Cell Physiol 209(2), 468-80.
180. Figge, M.T., et al. (2012) Deceleration of Fusion-Fission Cycles Improves Mitochondrial Quality Control during Aging. PLoS Comput Biol 8(6), e1002576.
181. Ashcroft, F.M. and P. Rorsman (2012) Diabetes mellitus and the beta cell: the last ten years. Cell 148(6), 1160-71.
182. Yoon, Y., et al. (2011) Mitochondrial dynamics in diabetes. Antioxid Redox Signal 14(3), 439-57.
183. Anello, M., et al. (2005) Functional and morphological alterations of mitochondria in pancreatic beta cells from type 2 diabetic patients. Diabetologia 48(2), 282-9.
184. Molina, A.J., et al. (2009) Mitochondrial networking protects beta-cells from nutrient-induced apoptosis. Diabetes 58(10), 2303-15.
185. Park, K.S., et al. (2008) Selective actions of mitochondrial fission/fusion genes on metabolism-secretion coupling in insulin-releasing cells. J Biol Chem 283(48), 33347-56.
186. Chen, H., J.M. McCaffery, and D.C. Chan (2007) Mitochondrial fusion protects against neurodegeneration in the cerebellum. Cell 130(3), 548-62.
187. Shutt, T.E. and H.M. McBride (2012) Staying cool in difficult times: Mitochondrial dynamics, quality control and the stress response. Biochim Biophys Acta.
188. Zhang, Z., et al. (2011) The dynamin-related GTPase Opa1 is required for glucose-stimulated ATP production in pancreatic beta cells. Mol Biol Cell 22(13), 2235-45.
189. Schon, E.A. and S. Przedborski (2011) Mitochondria: The Next (Neurode)Generation. Neuron 70(6), 1033-1053.
190. Zuchner, S., et al. (2004) Mutations in the mitochondrial GTPase mitofusin 2 cause Charcot-Marie-Tooth neuropathy type 2A. Nat Genet 36(5), 449-51.
191. Alexander, C., et al. (2000) OPA1, encoding a dynamin-related GTPase, is mutated in autosomal dominant optic atrophy linked to chromosome 3q28. Nat Genet 26(2), 211-5.
192. Delettre, C., et al. (2000) Nuclear gene OPA1, encoding a mitochondrial dynamin-related protein, is mutated in dominant optic atrophy. Nat Genet 26(2), 207-10.
193. Wang, X., et al. (2009) The role of abnormal mitochondrial dynamics in the pathogenesis of Alzheimer's disease. J Neurochem 109 Suppl 1, 153-9.

194. Wang, X., et al. (2008) Amyloid-beta overproduction causes abnormal mitochondrial dynamics via differential modulation of mitochondrial fission/fusion proteins. Proc Natl Acad Sci U S A 105(49), 19318-23.
195. Gilkerson, R.W., et al. (2012) Mitochondrial autophagy in cells with mtDNA mutations results from synergistic loss of transmembrane potential and mTORC1 inhibition. Hum Mol Genet 21(5), 978-90.
196. Xie, W. and K.K. Chung (2012) Alpha-synuclein impairs normal dynamics of mitochondria in cell and animal models of Parkinson's disease. J Neurochem.
197. Lin, X., et al. (2009) Leucine-rich repeat kinase 2 regulates the progression of neuropathology induced by Parkinson's-disease-related mutant alpha-synuclein. Neuron 64(6), 807-27.
198. Wang, X., et al. (2012) LRRK2 regulates mitochondrial dynamics and function through direct interaction with DLP1. Hum Mol Genet 21(9), 1931-44.
199. Wang, X., et al. (2012) Parkinson's disease-associated DJ-1 mutations impair mitochondrial dynamics and cause mitochondrial dysfunction. J Neurochem 121(5), 830-9.
200. Costa, V., et al. (2010) Mitochondrial fission and cristae disruption increase the response of cell models of Huntington's disease to apoptotic stimuli. EMBO Mol Med 2(12), 490-503.
201. Shirendeb, U., et al. (2011) Abnormal mitochondrial dynamics, mitochondrial loss and mutant huntingtin oligomers in Huntington's disease: implications for selective neuronal damage. Hum Mol Genet 20(7), 1438-55.
202. Song, W., et al. (2011) Mutant huntingtin binds the mitochondrial fission GTPase dynamin-related protein-1 and increases its enzymatic activity. Nat Med 17(3), 377-82.
203. Zhao, J., et al. (2009) The novel conserved mitochondrial inner-membrane protein MTGM regulates mitochondrial morphology and cell proliferation. J Cell Sci 122(Pt 13), 2252-62.
204. Chung, Y.M., J.S. Kim, and Y.D. Yoo (2006) A novel protein, Romo1, induces ROS production in the mitochondria. Biochem Biophys Res Commun 347(3), 649-55.
205. Hwang, I.T., et al. (2007) Drug resistance to 5-FU linked to reactive oxygen species modulator 1. Biochem Biophys Res Commun 359(2), 304-10.
206. Na, A.R., et al. (2008) A critical role for Romo1-derived ROS in cell proliferation. Biochem Biophys Res Commun 369(2), 672-8.
207. Chung, J.S., et al. (2009) Mitochondrial reactive oxygen species originating from Romo1 exert an important role in normal cell cycle progression by regulating p27(Kip1) expression. Free Radic Res 43(8), 729-37.
208. Lee, S.B., et al. (2011) Romo1 is a negative-feedback regulator of Myc. J Cell Sci 124(Pt 11), 1911-24.
209. Lee, S.B., et al. (2010) Serum deprivation-induced reactive oxygen species production is mediated by Romo1. Apoptosis 15(2), 204-18.
210. Kim, J.J., et al. (2010) TNF-alpha-induced ROS production triggering apoptosis is directly linked to Romo1 and Bcl-X(L). Cell Death Differ 17(9), 1420-34.

211. Chung, J.S., et al. (2012) Overexpression of Romo1 Promotes Production of Reactive Oxygen Species and Invasiveness of Hepatic Tumor Cells. Gastroenterology.
212. Chung, Y.M., et al. (2008) Replicative senescence induced by Romo1-derived reactive oxygen species. J Biol Chem 283(48), 33763-71.
213. Lee, S.B., et al. (2011) Bcl-XL prevents serum deprivation-induced oxidative stress mediated by Romo1. Oncol Rep 25(5), 1337-42.
214. Kaelin, W.G., Jr. (2012) Molecular biology. Use and abuse of RNAi to study mammalian gene function. Science 337(6093), 421-2.
215. Schauss, A.C., et al. (2010) A novel cell-free mitochondrial fusion assay amenable for high-throughput screenings of fusion modulators. BMC Biol 8, 100.
216. Nagahara, N. (2011) Intermolecular disulfide bond to modulate protein function as a redox-sensing switch. Amino Acids 41(1), 59-72.
217. Gebert, M., et al. (2012) Mgr2 promotes coupling of the mitochondrial presequence translocase to partner complexes. J Cell Biol 197(5), 595-604.
218. Chevrollier, A., et al. (2012) Standardized mitochondrial analysis gives new insights into mitochondrial dynamics and OPA1 function. Int J Biochem Cell Biol 44(6), 980-8.
219. (2003) Whither RNAi? Nat Cell Biol 5(6), 489-90.
220. Bohnert, M., et al. (2012) Role of MINOS in protein biogenesis of the mitochondrial outer membrane. Mol Biol Cell.
221. Zerbes, R.M., et al. (2012) Role of MINOS in Mitochondrial Membrane Architecture: Cristae Morphology and Outer Membrane Interactions Differentially Depend on Mitofilin Domains. J Mol Biol 422(2), 183-91.
222. van der Laan, M., et al. (2012) Role of MINOS in mitochondrial membrane architecture and biogenesis. Trends Cell Biol 22(4), 185-92.
223. Martinou, J.C. and R.J. Youle (2006) Which came first, the cytochrome c release or the mitochondrial fission? Cell Death Differ 13(8), 1291-5.
224. Suen, D.F., K.L. Norris, and R.J. Youle (2008) Mitochondrial dynamics and apoptosis. Genes Dev 22(12), 1577-90.
225. Youle, R.J., and Karbowski, M. (2005) Mitochondrial fission in apoptosis. Nature Reviews Molecular Cell Biology 6(8), 657-663.

Chapter 6 Appendices

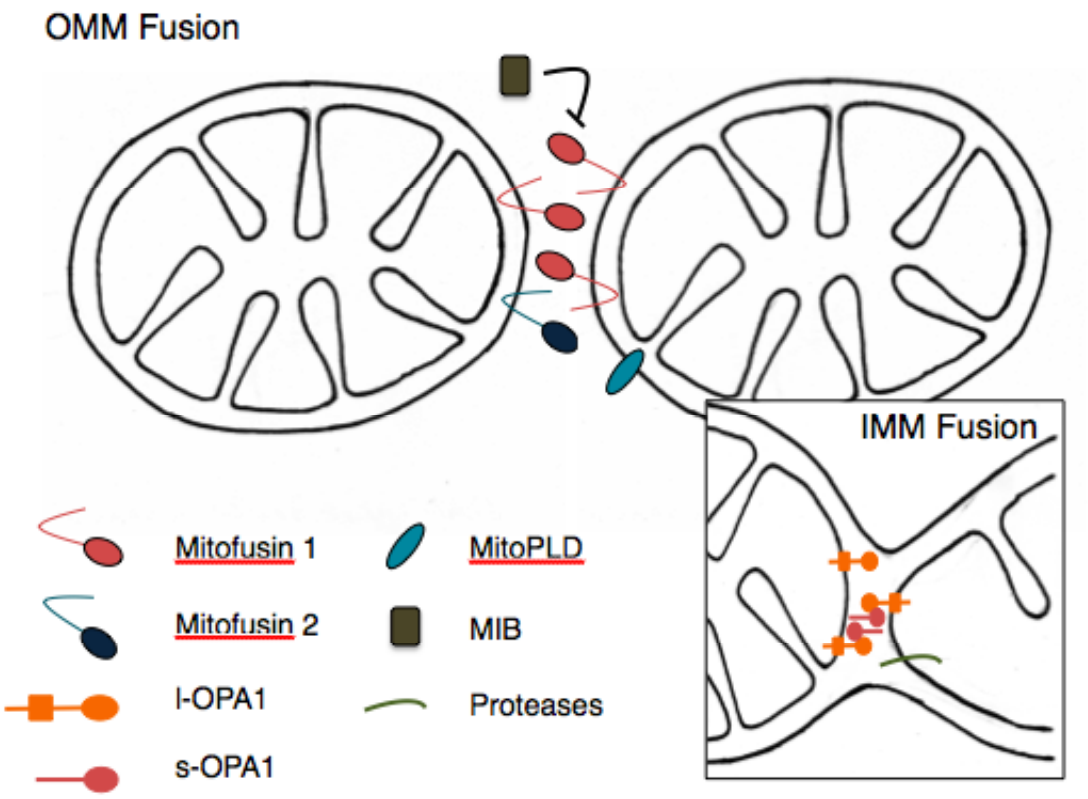

Appendix I Mammalian Outer and Inner Mitochondrial Fusion Machinery. Mitochondrial fusion is mediated in two steps. Fusion of the outer membrane, mediated by Mitofusin 1 and 2, and fusion of the inner membrane, mediated by long (l-OPA1) and short (s-OPA1) isoforms of OPA1.

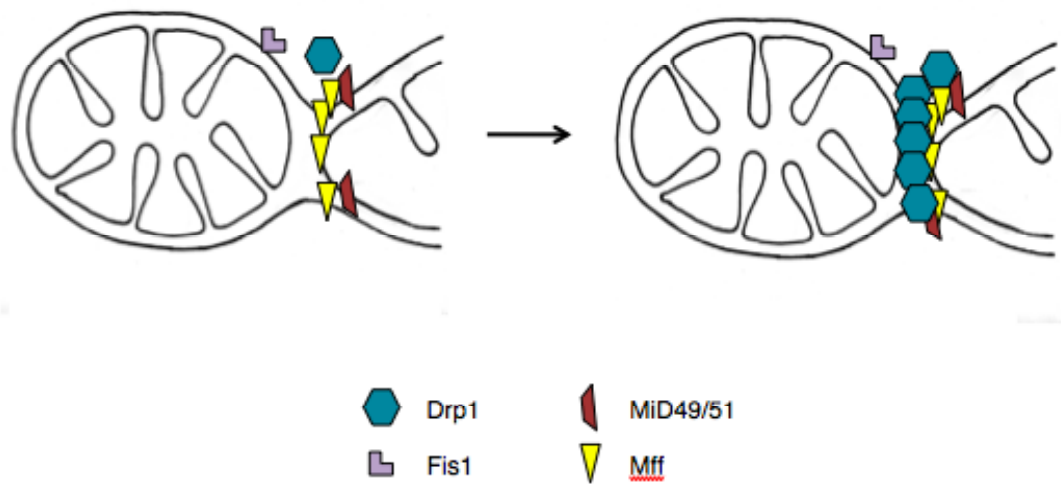

Appendix II Mammalian Mitochondrial Fission Machinery. Mitochondrial fission is mediated by the large GTPase, Drp1, which is recruited to the outer mitochondrial membrane by adaptor molecules, Mff and MiD49/51, where it oligomerizes into constriction rings.

MINOS	MICOS	MitOS	Mammalian Homologue
Fcj1	Fcj1	Fcj1	Mitofilin
Aim5	Mcs12	Aim5	
Mio10	Mcs10	Mos1	MINOS1
Aim13	Mcs19	Aim13	CHCHD3
Mio27	Mcs29	Mos2	
Aim37	Mcs27	Aim37	MOMA-1

Appendix III MINOS/MICOS/MitOS complex members and Mammalian Homologues.

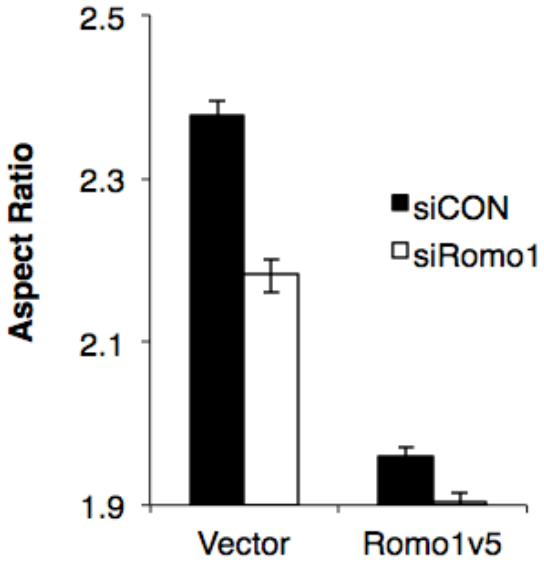

Appendix IV C-terminal tagged Romo1 acts as a dominant negative. Histogram showing aspect ratio of the mitochondrial networks of U20S cells transfected with siCON or siRomo1 and infected with lentivirus encoding either an empty vector or Romo1-v5.

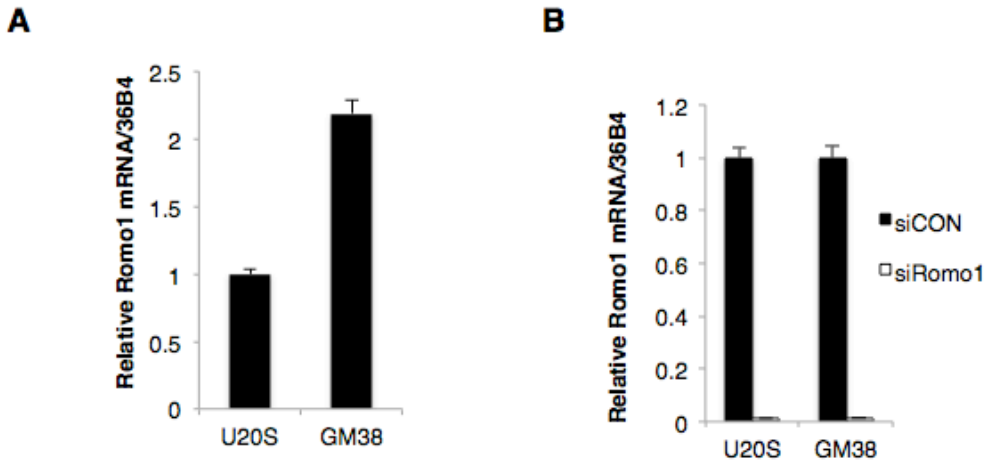

Appendix V Romo1 mRNA is present in both U20S and GM38 cells and is depleted by RNAi. A. RNA was collected from U20S and GM38 cells and qPCR analysis was performed to assess Romo1 mRNA expression in these cells. mRNA levels were normalized to the reference gene 36B4. B. RNA was collected from U20S and GM38 cells 72h after transfection of either siCON or siRomo1. qPCR analysis was performed to assess Romo1 mRNA expression in these cells. mRNA levels were normalized to the reference gene 36B4 and expressed relative to siCON of each cell line.

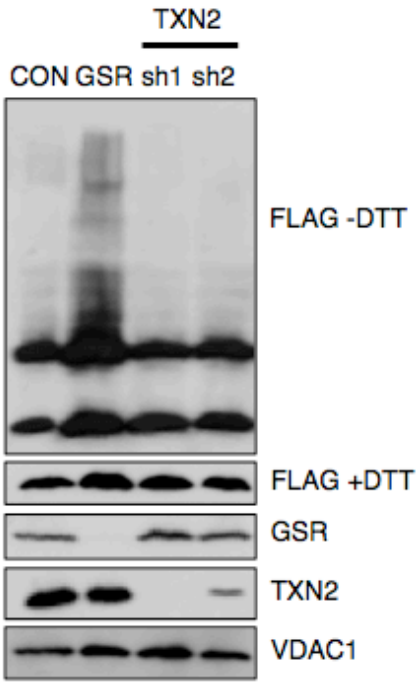

Appendix VI Romo1 REDOX status is regulated by glutathione reductase. Western blot of FLAG tagged ROMO1 WT following resolution on reducing (+DTT) and non-reducing (-DTT) gels, 96h after infection with lentivirus encoding shRNAs against CON, Gluathione reductase (GSR) or Thioredoxin 2 (TXN2). Western blot was also probed for GSR, TXN2 and VDAC1 as controls.

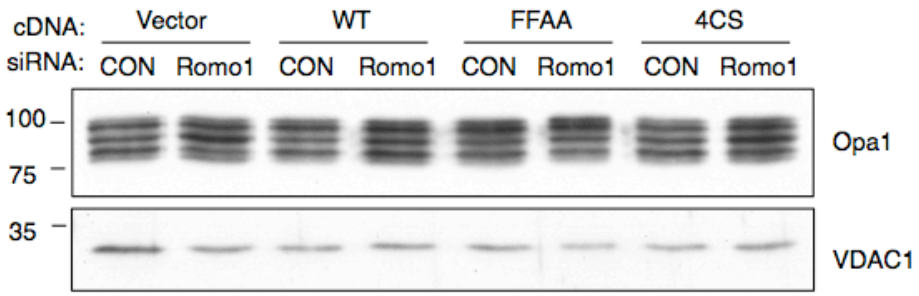

Appendix VII Cells lacking Romo1 display altered Opa1 processing. U20S were transfected with either siCON or siRomo1 and 4 hours later infected with lentivirus encoding either empty vector, siRNA-resistant Romo1 WT, -FFAA, or -4CS cDNA. Cell lysates were analyzed by SDS-PAGE and WB for Opa1 and VDAC1 as a loading control.

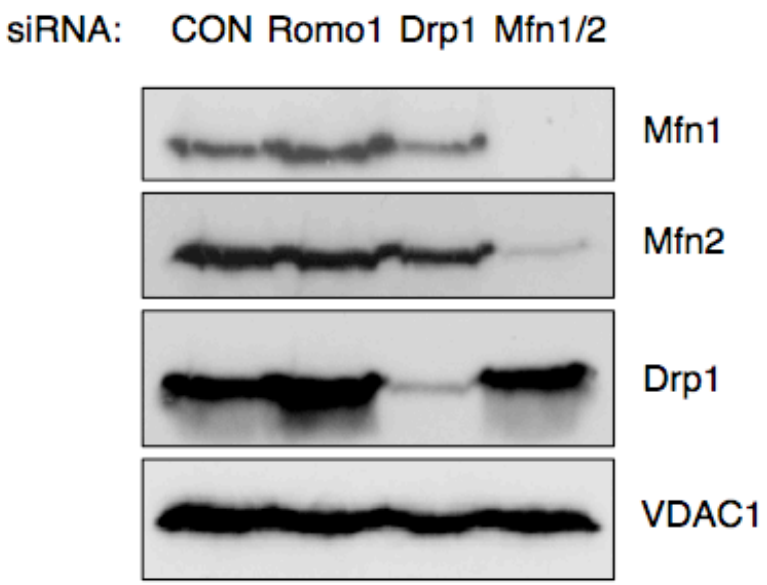

Appendix VIII Cells lacking Romo1 display normal expression of the Mitofusins and Drp1. U2OS cells were transfected with either siCON or siRNA targeting Romo1, Drp1, or Mfn1/2. Cell lysates were analyzed by SDS-PAGE and WB for Mfn1, Mfn2, Drp1 and VDAC1 as a loading control.

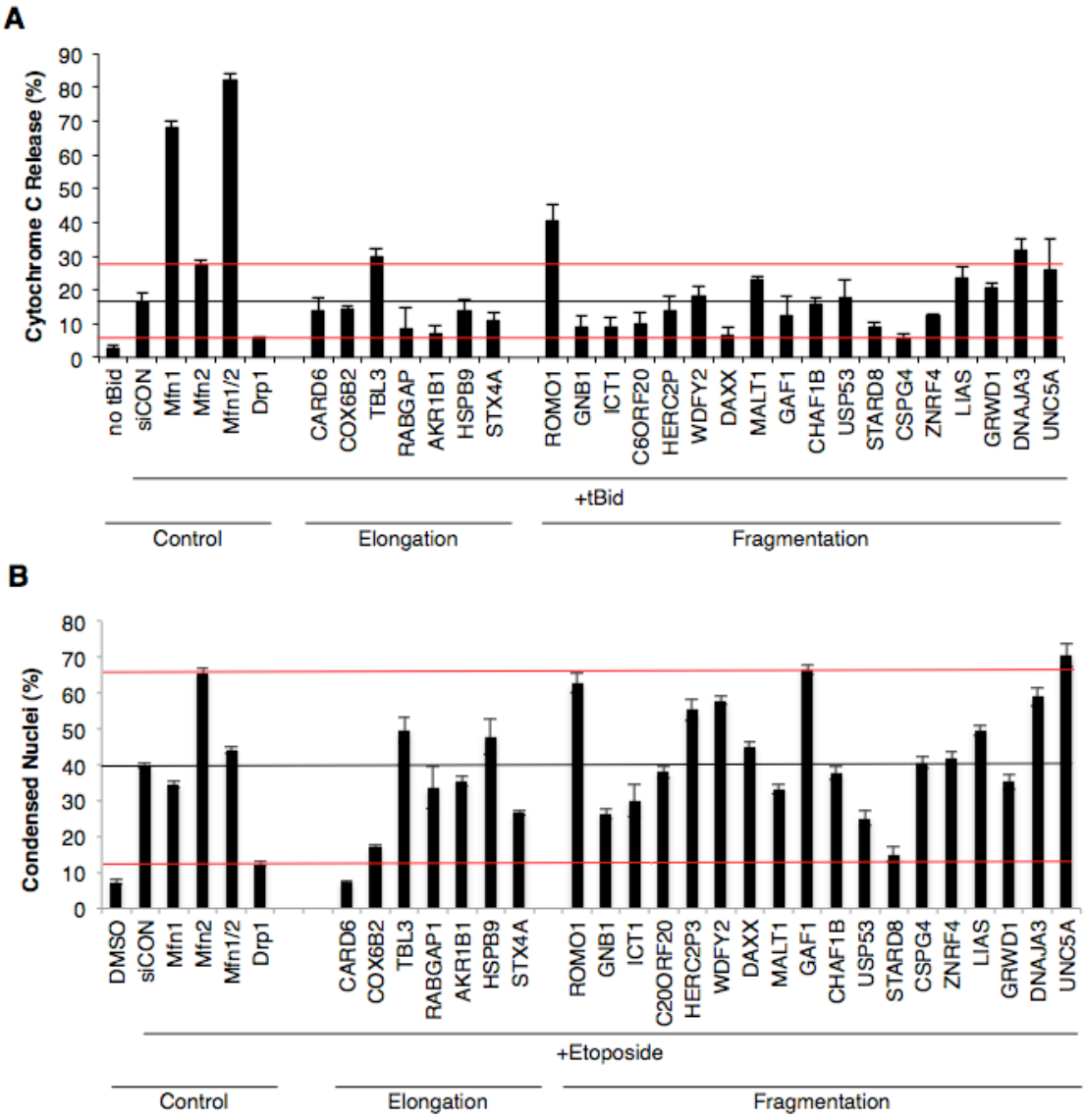

Appendix IX Uncoupling between mitochondrial morphology, cytochrome c release, and apoptosis. Deconvoluted siRNA targeting candidate genes from the morphology screen were transfected into U20S and treated with either Adeno-tBid for 8h (A) or 50uM etoposide for 20h (B). Cytochrome c release was measured in A, as decribed earlier. Apoptosis, as measured by condensed, apoptotic nuclear morphology, previously described, was measured in B. siRNA duplex yielding the most robust change in mitochondrial morphology is represented in histograms. Mfn1, Mfn2, Mfn1/2 and Drp1 are shown as controls.